Exploring the QGP at finite baryon chemical potential in and out of equilibrium

Elena Bratkovskaya

(GSI Darmstadt & Uni. Frankfurt)

Theoretical Physics Colloquium (on-line),

hosted by Prof. Igor Shovkovy at the Arizona State University.

20 January, 2021

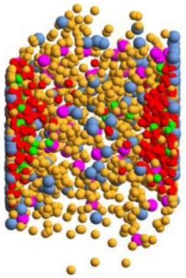

Experiment: Heavy-ion collisions

❑ Heavy-ion collision experiments

➔ ‚re-creation' of the Big Bang conditions in laboratory:
matter at high pressure and temperature

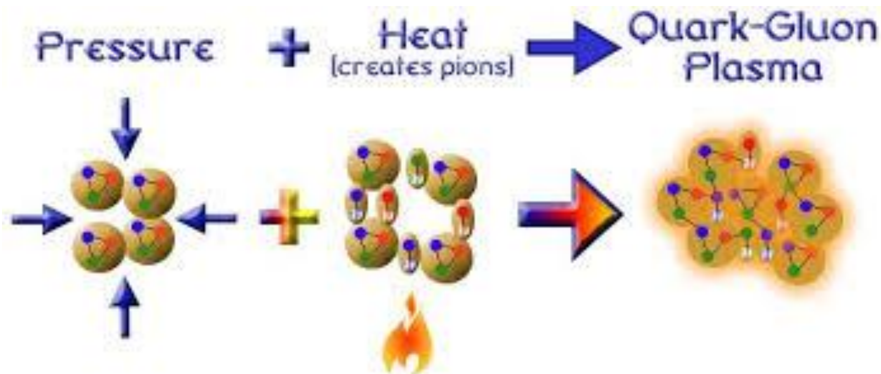

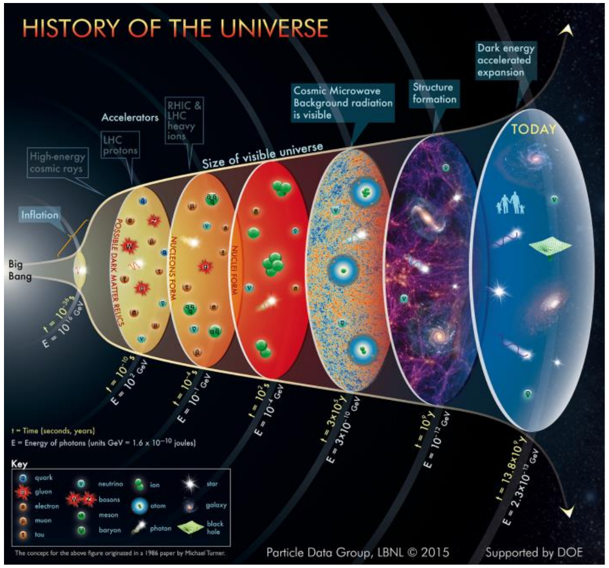

❑ Heavy-ion accelerators:

Large Hadron Collider - LHC (CERN):
Pb+Pb up to 574 A TeV

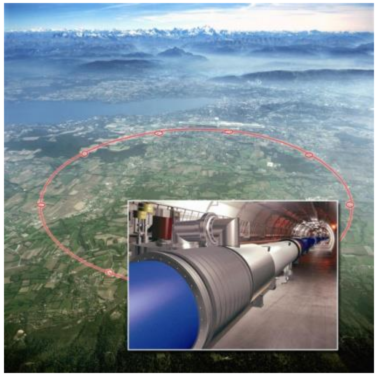

Relativistic-Heavy-Ion-Collider - RHIC (Brookhaven):
Au+Au up to 21.3 A TeV

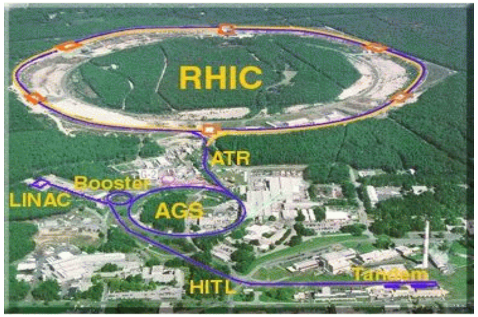

Facility for Antiproton and Ion Research – FAIR (Darmstadt)
(Under construction)
Au+Au up to 10 (30) A GeV

Nuclotron-based Ion Collider fAcility – NICA (Dubna)
(Under construction)
Au+Au up to 60 A GeV

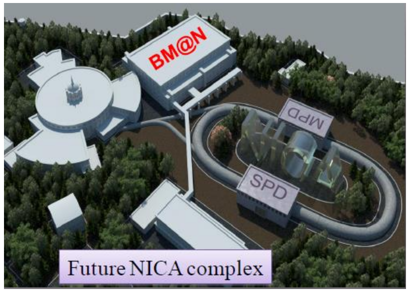

The ‚holy grail‘ of heavy-ion physics:

The phase diagram of QCD → thermal properties of QCD in the (T, μ_B) plain

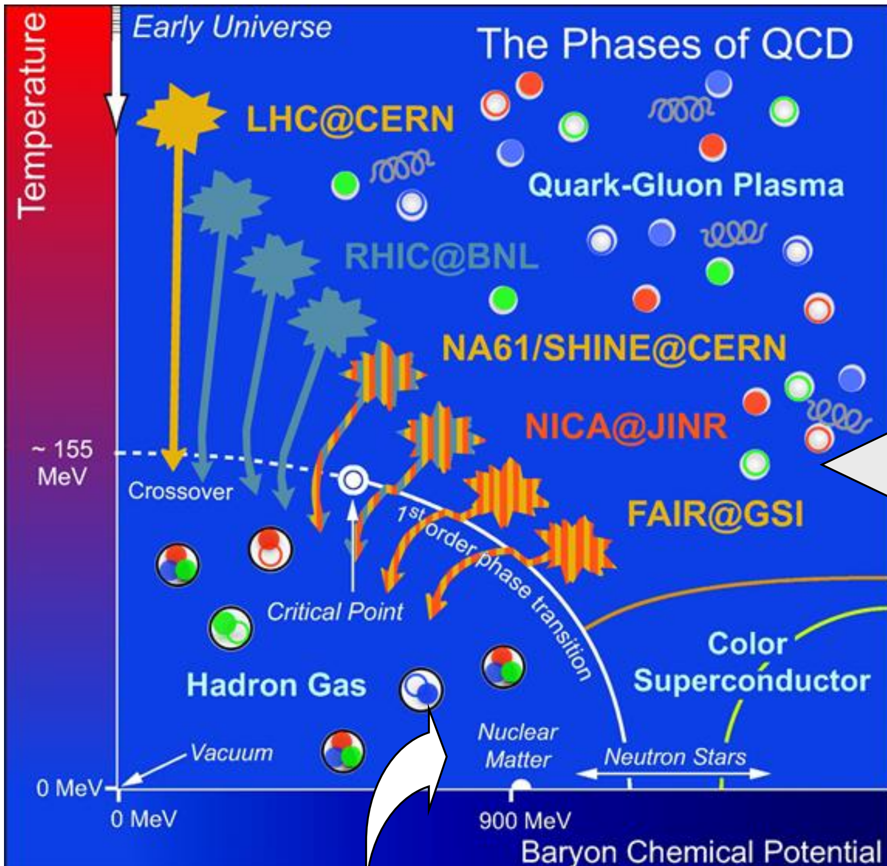

- **Equation-of-State of hot and dense matter?**
- **Study of the phase transition from hadronic to partonic matter – Quark-Gluon-Plasma**

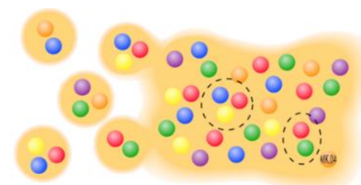

- **Search for a critical point**
- **Search for signatures of chiral symmetry restoration**

- **Study of the in-medium properties of hadrons at high baryon density and temperature**

Signals of the phase transition:

- Multi-strange particle enhancement in A+A
- Charm suppression
- Collective flow (v_1, v_2)
- Thermal dileptons
- Jet quenching and angular correlations
- High p_T suppression of hadrons
- Nonstatistical event-by-event fluctuations and correlations
- ...

Experiment: measures final hadrons and leptons

How to learn about physics from data?

Compare with theory!

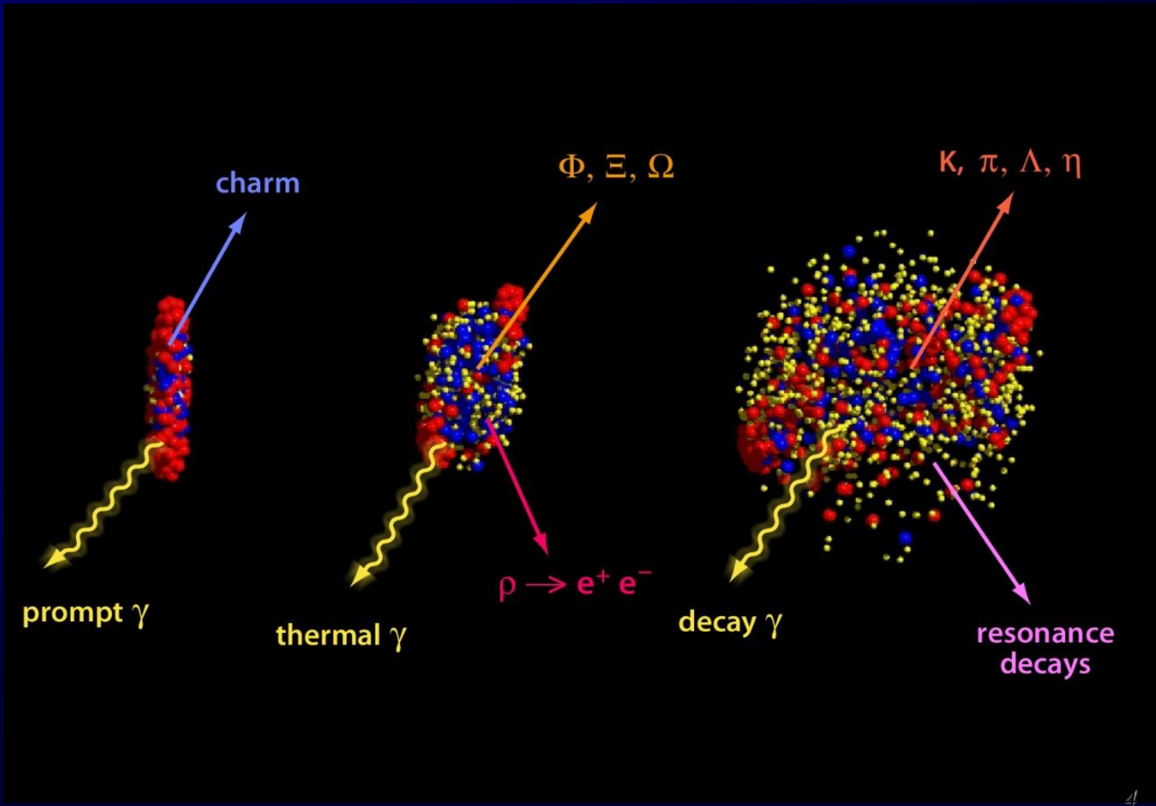

Basic models for heavy-ion collisions

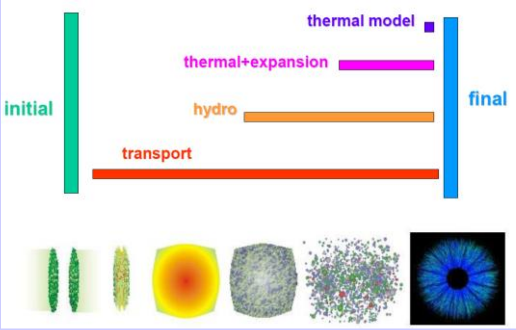

- **Statistical models:**

basic assumption: system is described by a (grand) canonical ensemble of non-interacting fermions and bosons in thermal and chemical equilibrium = thermal hadron gas at freeze-out with common T and μ_B

[- : no dynamical information]

- **Hydrodynamical models:**

basic assumption: conservation laws + equation of state (EoS); assumption of local thermal and chemical equilibrium
- Interactions are ‚hidden' in properties of the fluid described by transport coefficients (shear and bulk viscosity η, ζ, ..), which is 'input' for the hydro models

[- : simplified dynamics]

- **Microscopic transport models:**

based on transport theory of relativistic quantum many-body systems
- Explicitly account for the interactions of all degrees of freedom (hadrons and partons) in terms of cross sections and potentials
- Provide a unique dynamical description of strongly interaction matter in- and out-off equilibrium:
- In-equilibrium: transport coefficients are calculated in a box – controled by lQCD
- Nonequilibrium dynamics – controled by HIC

Actual solutions: Monte Carlo simulations

[+ : full dynamics | - : very complicated]

Microscopic modeling of HICs

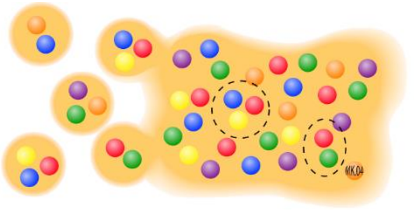

Goal: microscopic transport description of the partonic and hadronic phases of heavy-ion collisions

Problems:

- What are the properties of the QGP degrees of freedom?
- How to solve the hadronization problem?
- What is an appropriate transport theory ?

Information from lattice QCD at μ_B=0

I. deconfinement phase transition with increasing temperature + **II. chiral symmetry restoration with increasing temperature**

lQCD BMW collaboration: μ_B=0

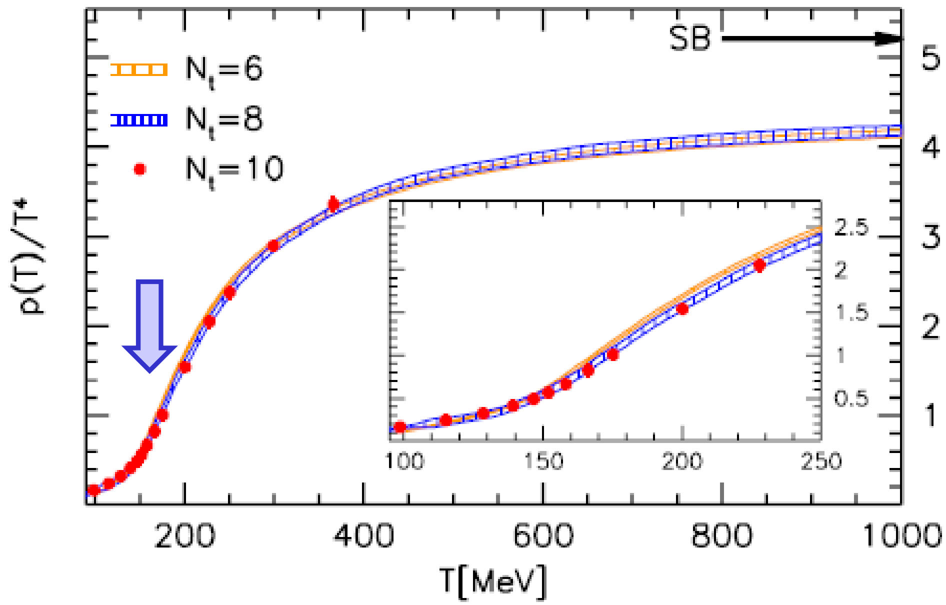

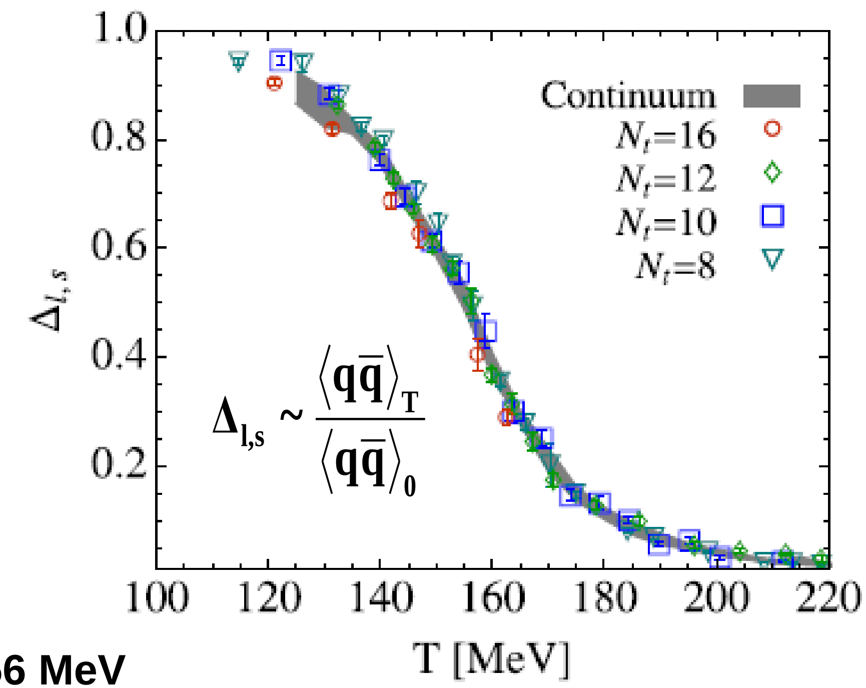

- **EoS: Crossover: hadron gas → QGP, T_C =156 MeV**

- **Scalar quark condensate $\langle\bar{q}q\rangle$ is viewed as an order parameter for the restoration of chiral symmetry:**

$$<\bar{q}q>= \begin{cases} \neq 0 & \text{chiral non-symmetric phase;} \\ = 0 & \text{chiral symmetric phase.} \end{cases}$$

➔ **both transitions occur at about the same temperature T_C for low chemical potentials**

Thermodynamics of QCD at finite T and μ_B

Theory: → thermal properties of QCD in the (T, μ_B) plain
→ lattice QCD – limited to low μ_B < 400 MeV - 'sign problem' of lQCD at finite μ_B

Taylor expansion allows for lQCD calculations for $\mu_q/T \ll 1$ $(\mu_B=3\mu_q)$

lQCD: J. Guenther et al., Nucl. Phys. A 967 (2017) 720

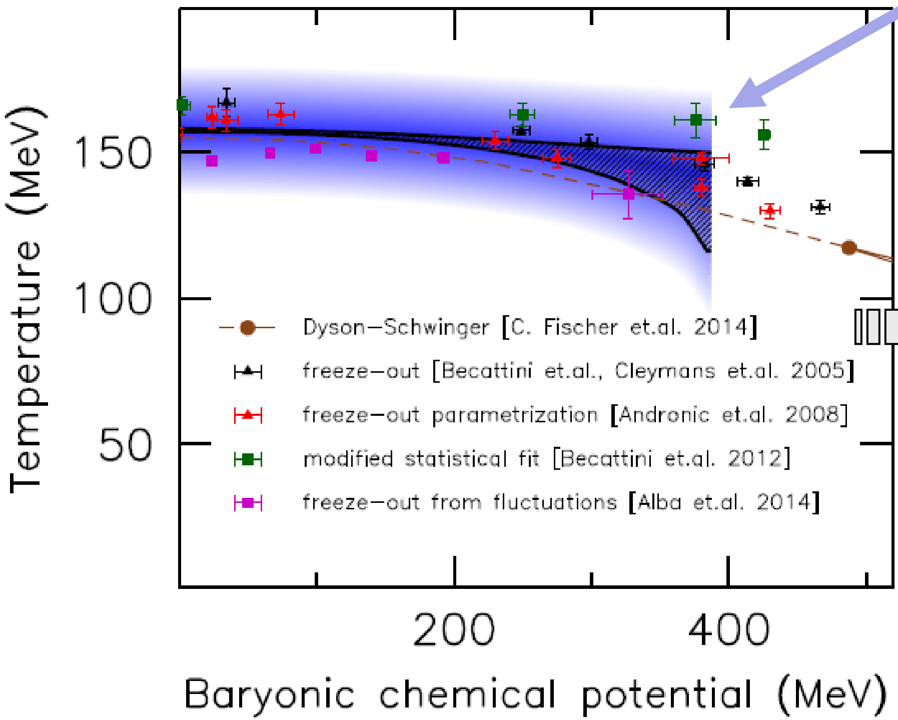

Possible phase diagram of QCD

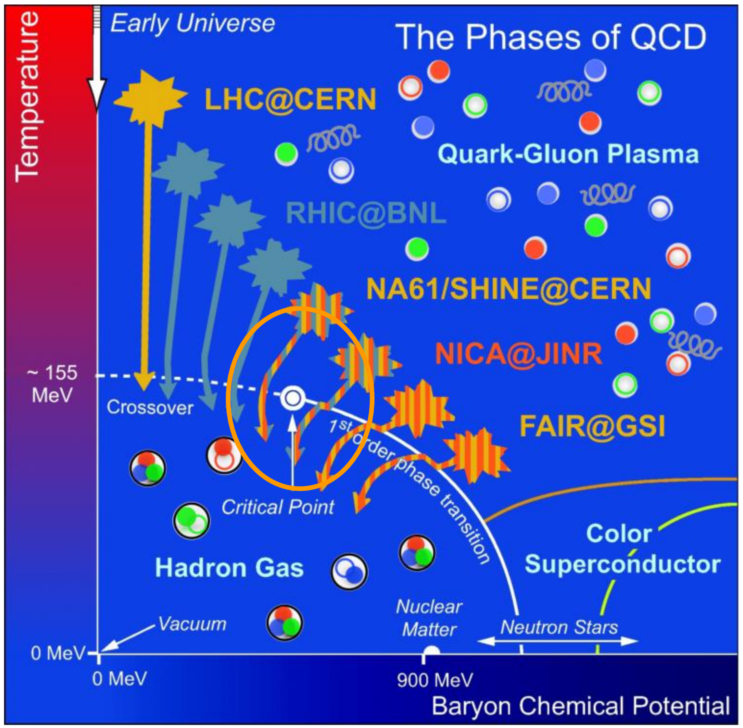

→ Lattice QCD results: up to $\mu_B < 400\ MeV$:
Crossover: hadron gas → QGP

Degrees-of-freedom of the QGP

For the microscopic transport description of the system one needs to know all degrees of freedom as well as their properties and interactions!

❖ lQCD gives QGP EoS at finite (T,μ_B)

! needs to be interpreted in terms of degrees-of-freedom

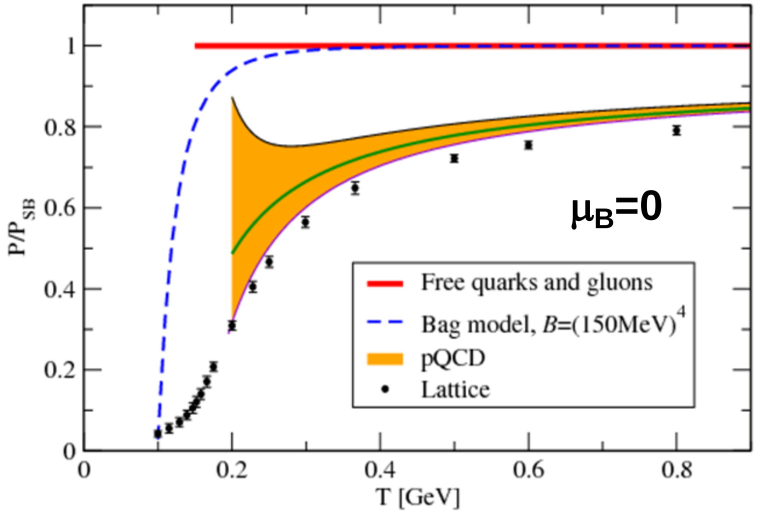

Non-perturbative QCD ← pQCD

pQCD:

- ❑ weakly interacting system
- ❑ massless quarks and gluons

Thermal QCD
= QCD at high parton densities:

- ❑ strongly interacting system
- ❑ massive quarks and gluons

➔ quasiparticles
= effective degrees-of-freedom

Present solution - effective models

DQPM (T, μ_q)

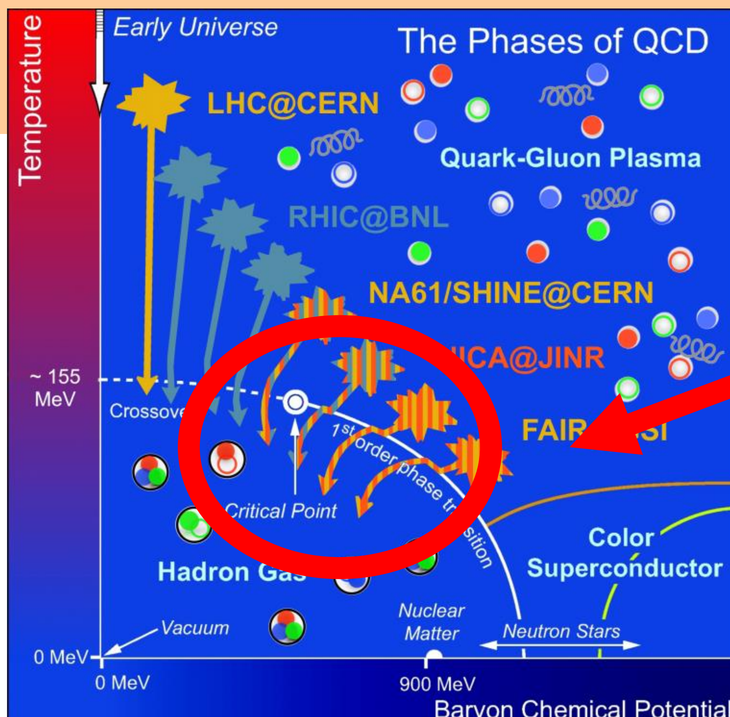

finite μ_q

Dynamical QuasiParticle Model (DQPM)

DQPM – effective model for the description of non-perturbative (strongly interacting) QCD based on lQCD EoS

Degrees-of-freedom: strongly interacting dynamical quasiparticles - quarks and gluons

Theoretical basis :

- ❑ **‚resummed' single-particle Green's functions → quark (gluon) propagator (2PI) :**

gluon propagator: $\Delta^{-1} = P^2 - \Pi$ &	quark propagator $S_q^{-1} = P^2 - \Sigma_q$
gluon self-energy: $\Pi = M_g^2 - i2\gamma_g\omega$ &	quark self-energy: $\Sigma_q = M_q^2 - i2\gamma_q\omega$

Properties of the quasiparticles are specified by scalar complex self-energies:

$Re\Sigma_q$: **thermal masses** (M_g, M_q); $Im\Sigma_q$: **interaction widths** (γ_g, γ_q)

→ **spectral functions** $\rho_q = -2ImS_q$ → **Lorentzian form:**

$$\rho_j(\omega, \mathbf{p}) = \frac{\gamma_j}{\tilde{E}_j}\left(\frac{1}{(\omega - \tilde{E}_j)^2 + \gamma_j^2} - \frac{1}{(\omega + \tilde{E}_j)^2 + \gamma_j^2}\right)$$

$$\equiv \frac{4\omega\gamma_j}{\left(\omega^2 - \mathbf{p}^2 - M_j^2\right)^2 + 4\gamma_j^2\omega^2} \qquad \tilde{E}_j^2(\mathbf{p}) = \mathbf{p}^2 + M_j^2 - \gamma_j^2$$

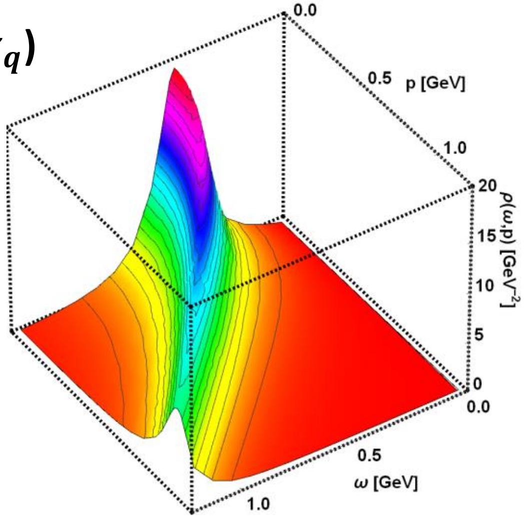

A. Peshier, W. Cassing, PRL 94 (2005) 172301; W. Cassing, NPA 791 (2007) 365: NPA 793 (2007), H. Berrehrah et al, Int.J.Mod.Phys. E25 (2016) 1642003; P. Moreau et al., PRC100 (2019) 014911; O. Soloveva et al., PRC101 (2020) 045203

Dynamical QuasiParticle Model (DQPM)

Theoretical basis → realization :

- introduce an ansatz (HTL; with few parameters) for the (T, μ_B) dependence of masses/widths
- ansatz for coupling constant *g* based on the lQCD entropy density as a function of T at μ_B=0
- scaling hypothesis for critical temperature $T_c(\mu_q)$:
- evaluate the QGP thermodynamics in equilibrium using the Kadanoff-Baym theory
- fix DQPM parameters by comparison to the entropy density s, pressure P, energy density ε from DQPM to lQCD results at μ_B =0

→ obtain the properties of the QGP at (T, μ_B)

A. Peshier, W. Cassing, PRL 94 (2005) 172301; W. Cassing, NPA 791 (2007) 365: NPA 793 (2007), H. Berrehrah et al, Int.J.Mod.Phys. E25 (2016) 1642003; P. Moreau et al., PRC100 (2019) 014911; O. Soloveva et al., PRC101 (2020) 045203

Parton properties

- Modeling of the quark/gluon masses and widths (inspired by HTL calculations)

Masses:

$$M^2_{q(\bar{q})}(T,\mu_B) = \frac{N_c^2-1}{8N_c} g^2(T,\mu_B)\left(T^2+\frac{\mu_q^2}{\pi^2}\right)$$

$$M^2_g(T,\mu_B) = \frac{g^2(T,\mu_B)}{6}\left(\left(N_c+\frac{1}{2}N_f\right)T^2+\frac{N_c}{2}\sum_q\frac{\mu_q^2}{\pi^2}\right)$$

Widths:

$$\gamma_{q(\bar{q})}(T,\mu_B) = \frac{1}{3}\frac{N_c^2-1}{2N_c}\frac{g^2(T,\mu_B)T}{8\pi}\ln\left(\frac{2c}{g^2(T,\mu_B)}+1\right)$$

$$\gamma_g(T,\mu_B) = \frac{1}{3}N_c\frac{g^2(T,\mu_B)T}{8\pi}\ln\left(\frac{2c}{g^2(T,\mu_B)}+1\right)$$

➔ **DQPM :**
only one parameter (c = 14.4) + (T,μ_B)- dependent coupling constant has to be determined from lattice results

- **Coupling g:** input - lQCD entropy density s function of T at μ_B=0

$$g^2(s/s_{SB}) = d\left((s/s_{SB})^e-1\right)^f$$

$$s_{SB}^{QCD} = 19/9\pi^2T^3$$

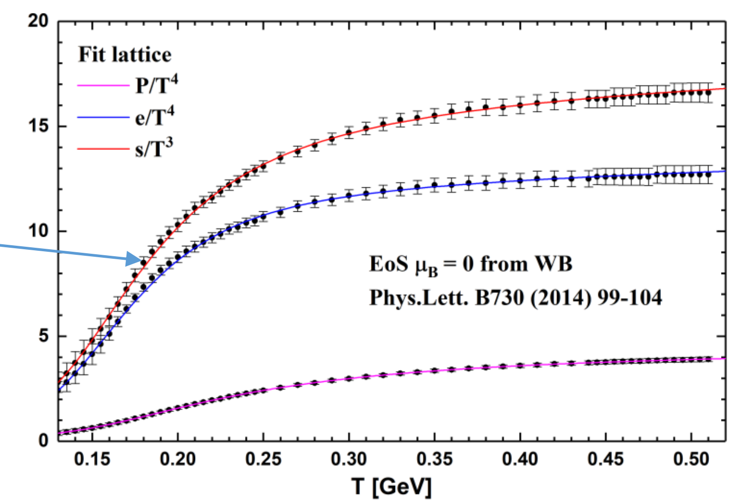

H. Berrehrah et al, PRC 93 (2016) 044914,
Int.J.Mod.Phys. E25 (2016) 1642003,

DQPM at finite (T, μ_q): scaling hypothesis

- **Scaling hypothesis for the effective temperature T***
  for $N_f = N_c = 3$

$$\mu_u = \mu_d = \mu_s = \mu_q$$

$$\boxed{T^{*2} = T^2 + \frac{\mu_q^2}{\pi^2}}$$

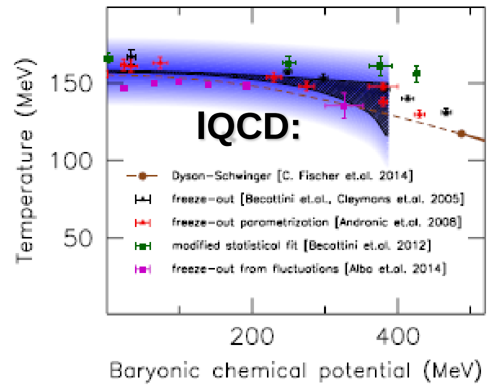

- **Coupling:**

$$g(T/T_c(\mu=0)) \longrightarrow g(T^\star/T_c(\mu))$$

- **Critical temperature $T_c(\mu_q)$:**
  obtained by assuming a constant energy density ε for the system at $T=T_c(\mu_q)$, where ε at $T_c(\mu_q=0)$=156 GeV is fixed by lQCD at μ_q=0

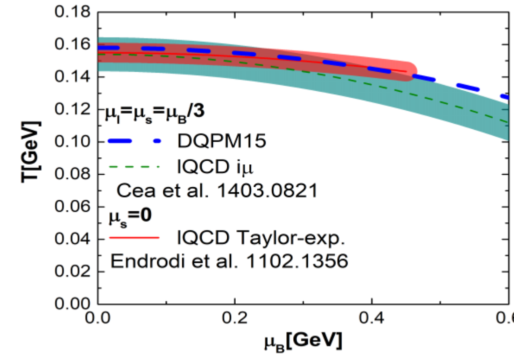

$$\boxed{\frac{T_c(\mu_q)}{T_c(\mu_q=0)} = \sqrt{1-\alpha\,\mu_q^2} \approx 1-\alpha/2\,\mu_q^2+\cdots}$$

$$\alpha \approx 8.79\ \mathrm{GeV}^{-2}$$

! Consistent with lattice QCD:

lQCD: C. Bonati et al., PRC90 (2014) 114025

$$\frac{T_c(\mu_B)}{T_c} = 1-\kappa\left(\frac{\mu_B}{T_c}\right)^2+\cdots$$

lQCD $\kappa = 0.013(2)$ ⟷ $\kappa_{DQPM} \approx 0.0122$

H. Berrehrah et al, PRC 93 (2016) 044914, Int.J.Mod.Phys. E25 (2016) 1642003,

DQPM thermodynamics at finite (T, μ_q)

- **Entropy and baryon density** in the quasiparticle limit (G. Baym 1998):

$$
\begin{aligned}
s^{dqp} = \\
& - \int \frac{d\omega}{2\pi} \frac{d^3p}{(2\pi)^3} \left[d_g \frac{\partial n_B}{\partial T} \left(\mathrm{Im}(\ln -\Delta^{-1}) + \mathrm{Im}\,\Pi\, \mathrm{Re}\,\Delta \right) \right. \\
& + \sum_{q=u,d,s} d_q \frac{\partial n_F(\omega-\mu_q)}{\partial T} \left(\mathrm{Im}(\ln -S_q^{-1}) + \mathrm{Im}\,\Sigma_q\, \mathrm{Re}\, S_q \right) \\
& \left. + \sum_{\bar{q}=\bar{u},\bar{d},\bar{s}} d_{\bar{q}} \frac{\partial n_F(\omega+\mu_q)}{\partial T} \left(\mathrm{Im}(\ln -S_{\bar{q}}^{-1}) + \mathrm{Im}\,\Sigma_{\bar{q}}\, \mathrm{Re}\, S_{\bar{q}} \right) \right]
\end{aligned}
$$

$$
\begin{aligned}
n^{dqp} = - \int \frac{d\omega}{2\pi} \frac{d^3p}{(2\pi)^3} \\
& \left[\sum_{q=u,d,s} d_q \frac{\partial n_F(\omega-\mu_q)}{\partial \mu_q} \left(\mathrm{Im}(\ln -S_q^{-1}) + \mathrm{Im}\,\Sigma_q\, \mathrm{Re}\, S_q \right) \right. \\
& \left. + \sum_{\bar{q}=\bar{u},\bar{d},\bar{s}} d_{\bar{q}} \frac{\partial n_F(\omega+\mu_q)}{\partial \mu_q} \left(\mathrm{Im}(\ln -S_{\bar{q}}^{-1}) + \mathrm{Im}\,\Sigma_{\bar{q}}\, \mathrm{Re}\, S_{\bar{q}} \right) \right]
\end{aligned}
$$

Blaizot, Iancu, Rebhan, Phys. Rev. D 63 (2001) 065003

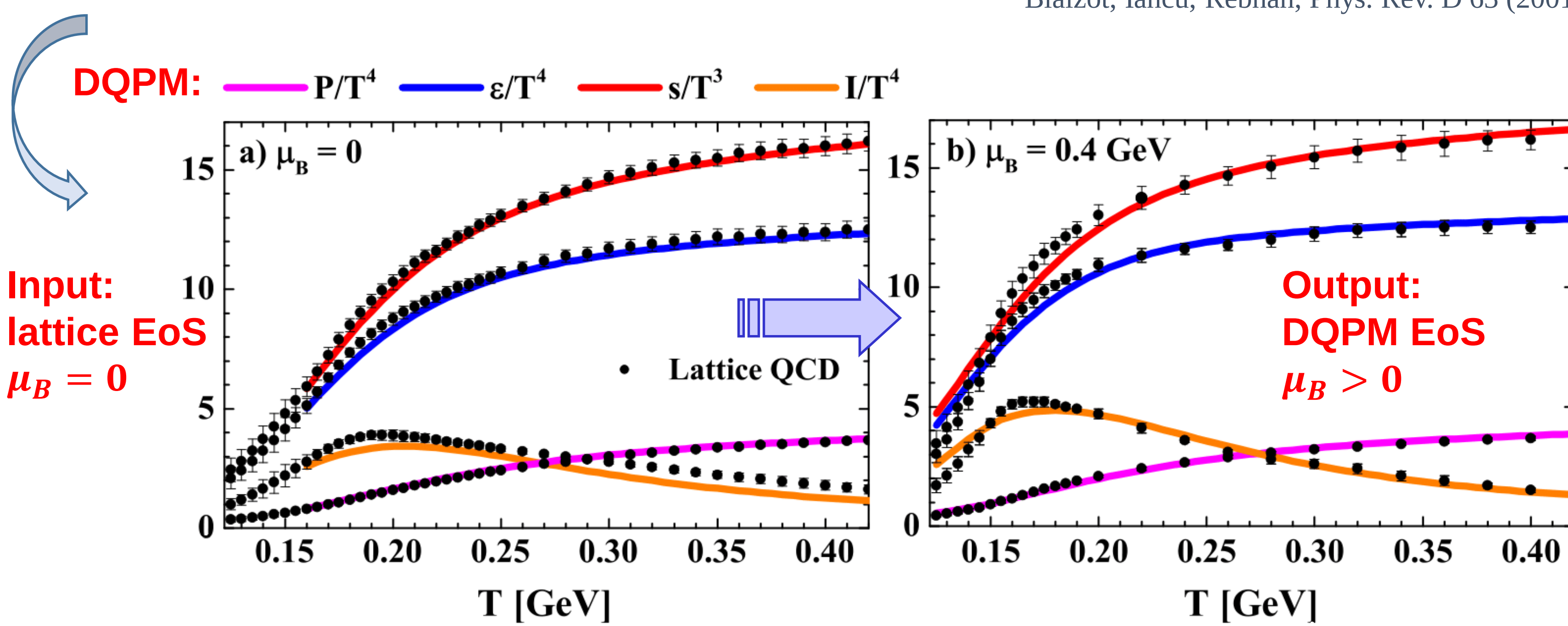

lQCD: Sz. Borsanyi et al., JHEP 1208 (2012) 053

DQPM: parton properties

- Coupling as a function of (T, μ_B)

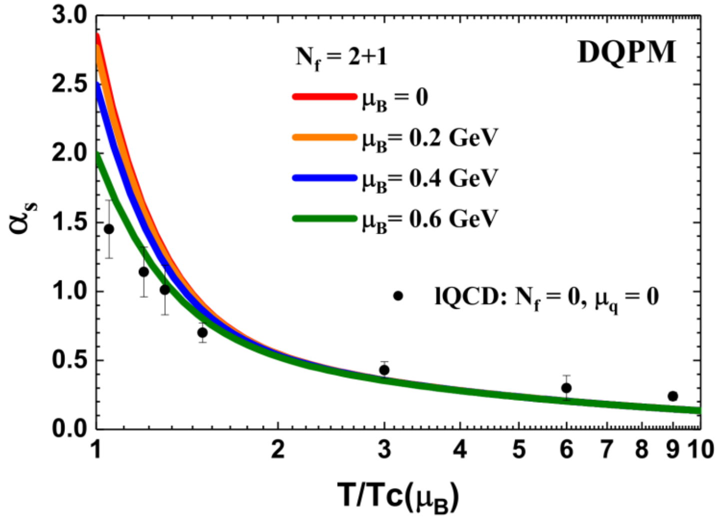

→ **Lorentzian spectral function:**

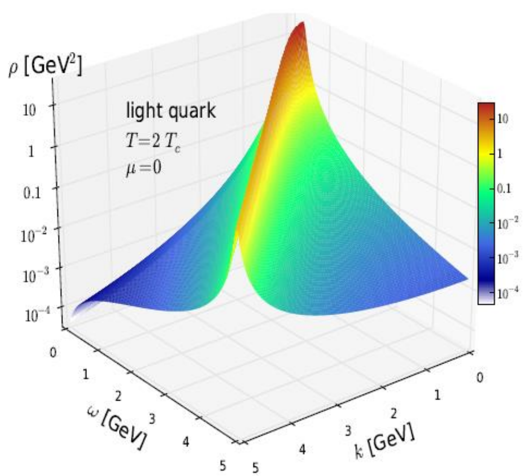

- Masses and widths as a function of (T, μ_B)

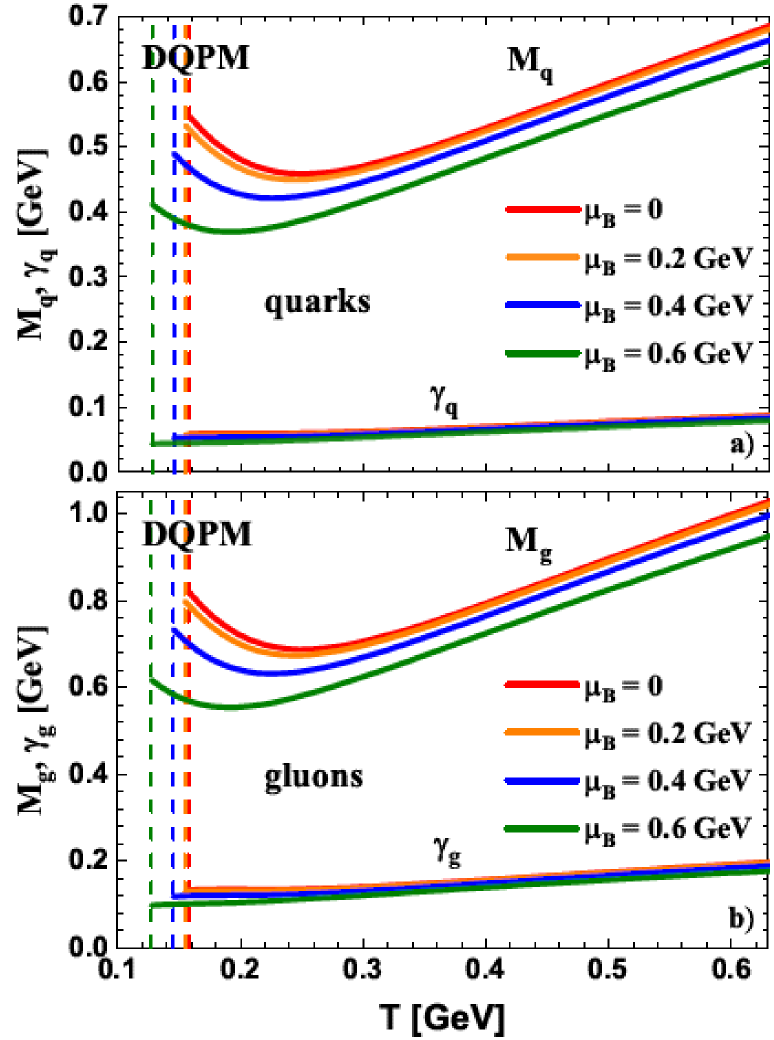

P. Moreau et al., PRC100 (2019) 014911

Partonic interactions: matrix elements

DQPM partonic cross sections → leading order diagrams

- **Propagators for massive bosons and fermions:**

$$= -i\delta_{ab}\frac{g^{\mu\nu} - q^\mu q^\nu / M_g^2}{q^2 - M_g^2 + 2i\gamma_g q_0}$$

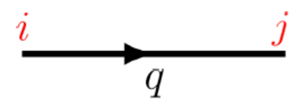

$$= i\delta_{ij}\frac{\not{q} + M_q}{q^2 - M_q^2 + 2i\gamma_q q_0}$$

qq' → qq' scattering

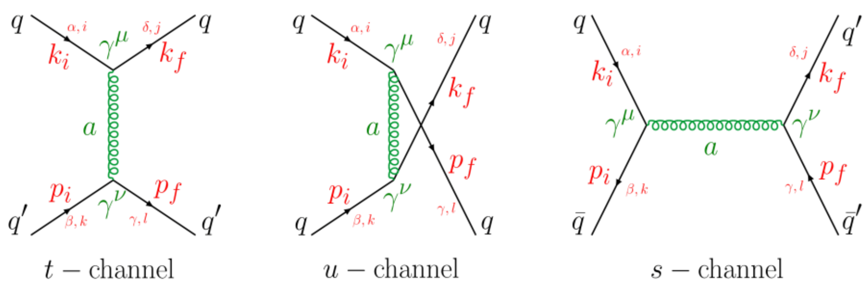

gq → gq scattering

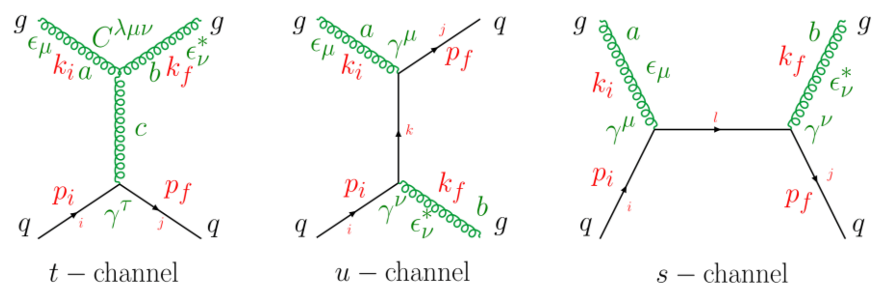

gg → gg scattering

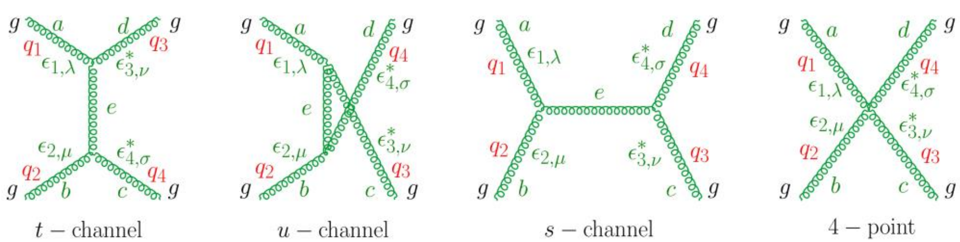

H. Berrehrah et al, PRC 93 (2016) 044914, Int.J.Mod.Phys. E25 (2016) 1642003, → **P. Moreau et al., PRC100 (2019) 014911**

Differential cross sections

- **On-shell:**

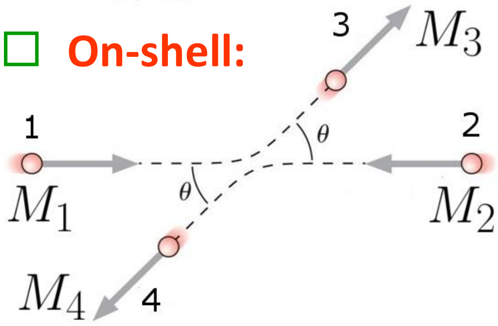

Initial masses: pole masses
Final masses: pole masses

- **Off-shell:**

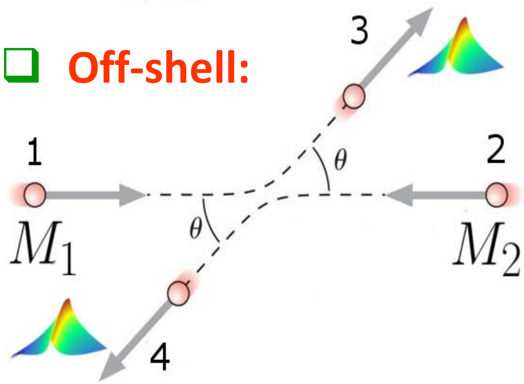

Initial masses: pole masses
Final masses: integrated over spectral functions

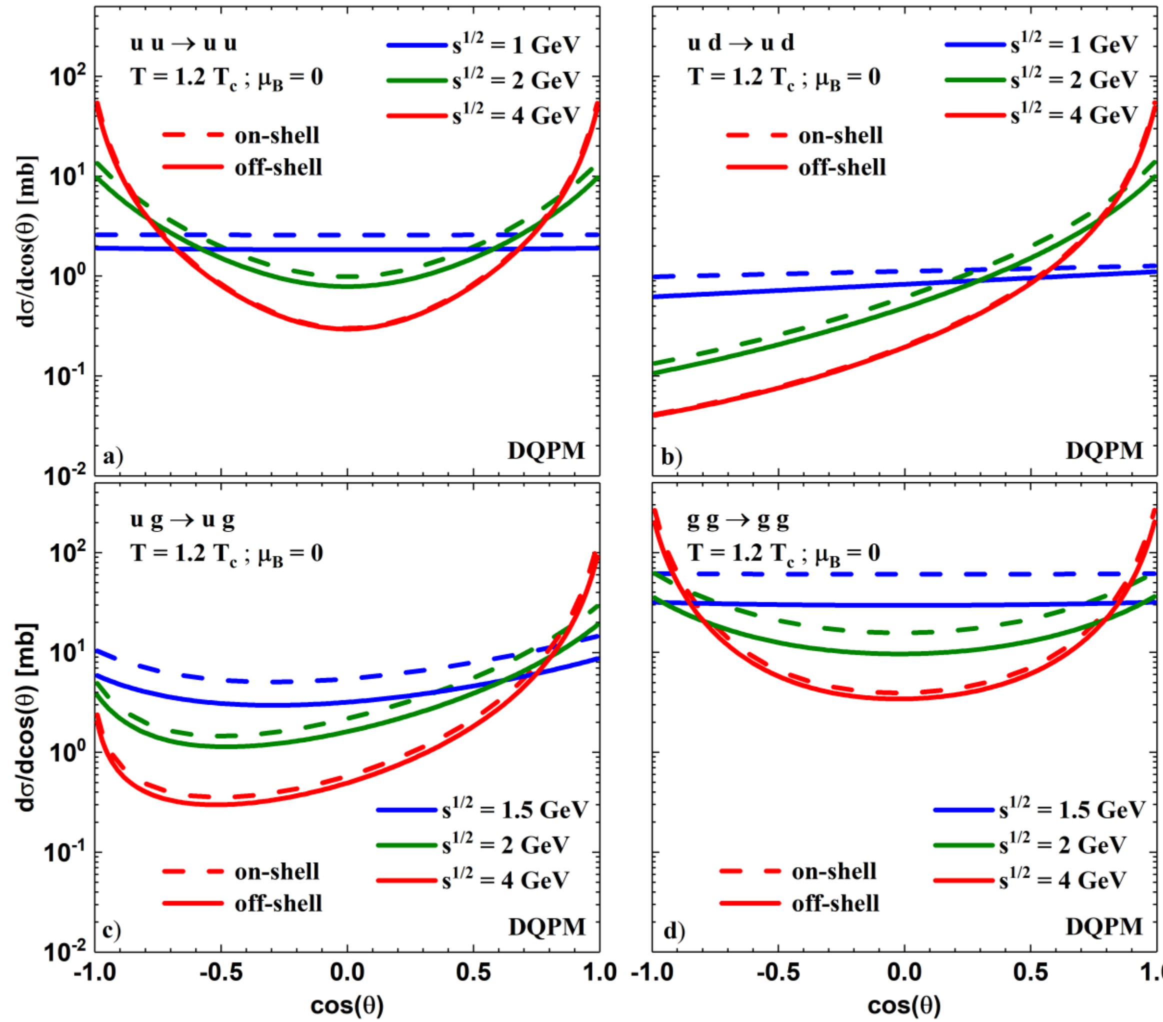

- **At lower s: off-shell σ < on -shell σ since $\omega_3 + \omega_4 < \sqrt{s}$**

P. Moreau et al., PRC100 (2019) 014911

Total cross section

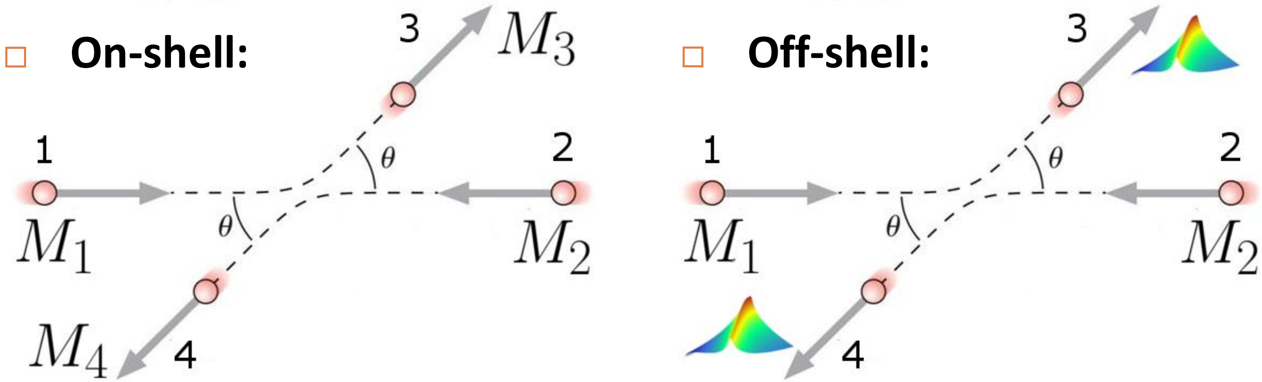

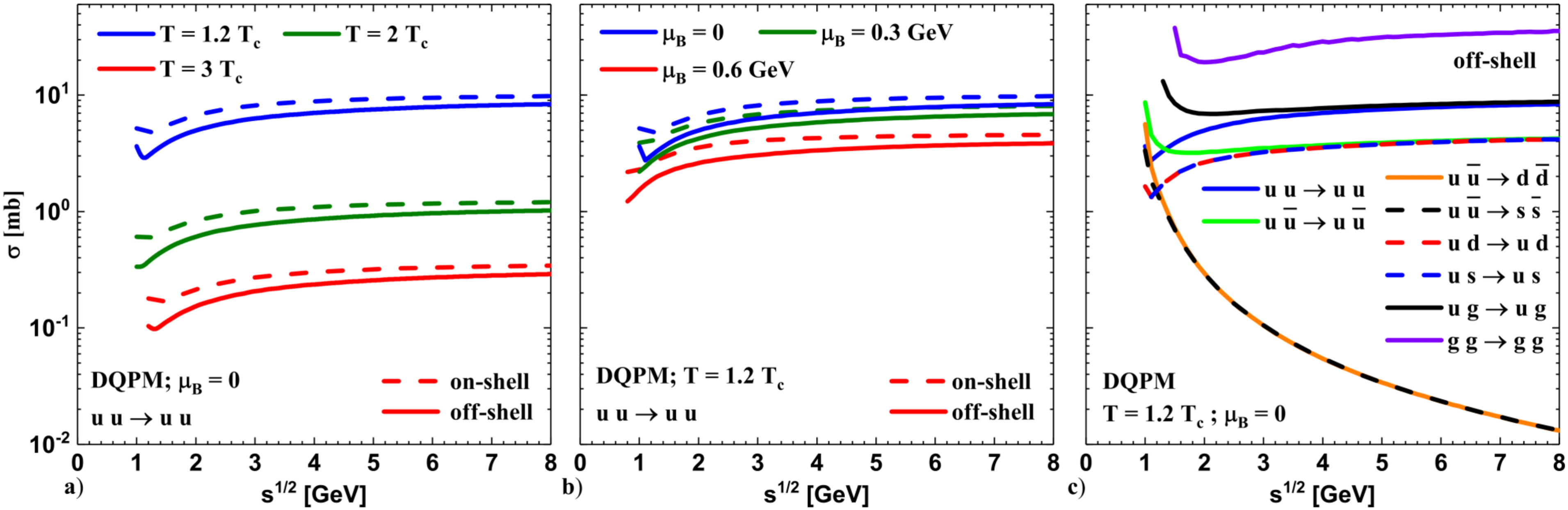

P. Moreau et al., PRC100 (2019) 014911

DQPM: Mean-field potential for quasiparticles

Space-like part of energy-momentum tensor $T_{\mu\nu}$ defines the potential energy density:

$$V_p(T,\mu_q) = T^{00}_{g-}(T,\mu_q) + T^{00}_{q-}(T,\mu_q) + T^{00}_{\bar{q}-}(T,\mu_q)$$

space-like gluons + space-like quarks+antiquarks

$$\tilde{\mathrm{Tr}}_g^{\pm} \cdots = d_g \int \frac{d\omega}{2\pi} \frac{d^3p}{(2\pi)^3} 2\omega\, \rho_g(\omega)\, \Theta(\omega)\, n_B(\omega/T)\, \Theta(\pm P^2) \cdots$$

$$\tilde{\mathrm{Tr}}_q^{\pm} \cdots = d_q \int \frac{d\omega}{2\pi} \frac{d^3p}{(2\pi)^3} 2\omega\, \rho_q(\omega)\, \Theta(\omega)\, n_F((\omega-\mu_q)/T)\, \Theta(\pm P^2) \cdots$$

$$\tilde{\mathrm{Tr}}_{\bar{q}}^{\pm} \cdots = d_{\bar{q}} \int \frac{d\omega}{2\pi} \frac{d^3p}{(2\pi)^3} 2\omega\, \rho_{\bar{q}}(\omega)\, \Theta(\omega)\, n_F((\omega+\mu_q)/T)\, \Theta(\pm P^2) \cdots$$

➔ **mean-field scalar potential (1PI) for quarks and gluons (U_q, U_g) vs parton scalar density ρ_S:**

$$U_s(\rho_s) = \frac{dV_p(\rho_s)}{d\rho_s} \qquad \rho_S = N_g^+ + N_q^+ + N_{\bar{q}}^+$$

$$Uq = Us, \quad Ug \sim 2Us$$

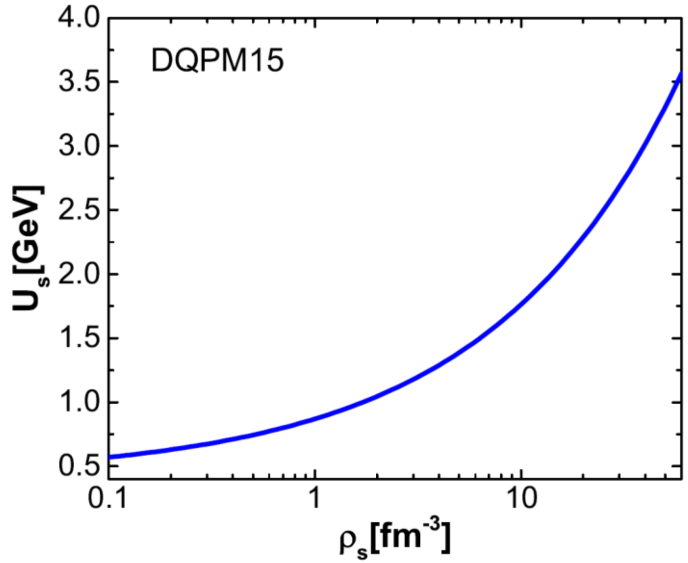

Quasiparticle potentials (U_q, U_g) are repulsive !

➔ **the force acting on a quasiparticle j:**

$$F \sim M_j/E_j \nabla U_s(x) = M_j/E_j\; dU_s/d\rho_s\; \nabla\rho_s(x)$$

$$j = g, q, \bar{q}$$

➔ **accelerates particles**

Cassing, NPA 791 (2007) 365: NPA 793 (2007)

QGP near equilibrium

DQPM (T, μ_q) :

transport properties at finite (T, μ_q)

The properties of QGP in HICs → transport coefficients

Properties of the QGP near equilibrium are characterized by transport coefficients

Shear η, bulk viscosity ζ , … are ‘input’ for the viscous hydrodynamic models!

Hydrodynamics

$$T^{\mu\nu} = -Pg^{\mu\nu} + wu^\mu u^\nu + \Delta T^{\mu\nu}$$

$$J_B^\mu = n_B u^\mu + \Delta J_B^\mu$$

$$\begin{cases} \partial_\mu J_B^\mu = 0 \\ \partial_\mu T^{\mu\nu} = 0 \end{cases}$$

input for hydro simulations

$$\Delta T^{\mu\nu} = \boxed{\eta}\left(D^\mu u^\nu + D^\nu u^\mu + \tfrac{2}{3}\Delta^{\mu\nu}\partial_\rho u^\rho\right) - \boxed{\zeta}\Delta^{\mu\nu}\partial_\rho u^\rho$$

$$\Delta J_B^\mu = \boxed{\kappa_B} D^\mu\left(\frac{\mu_B}{T}\right)$$

$$D^\mu = \Delta^{\alpha\nu}\partial_\nu \qquad \Delta^{\mu\nu} = g^{\mu\nu} - u^\mu u^\nu$$

Shear viscosity
Resistance to ‘deformation’
$\eta \bigtriangledown^{<\mu} u^{\nu>}$

Bulk viscosity
Resistance to expansion
$-\zeta \bigtriangledown u$

Baryon/electric charge
diffusion coefficients
$\kappa_B \bigtriangledown^\mu \frac{\mu_B}{T}$

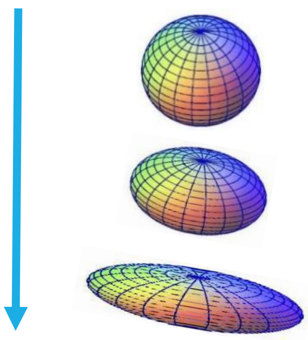

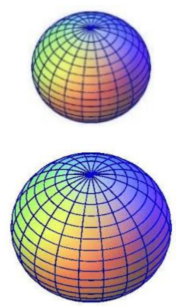

The properties of QGP from HIC - shear viscosity

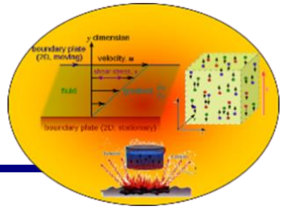

The **shear viscosity** of a system measures its **resistance** to flow.

Wikipedia: Viscosity can be conceptualized as quantifying the **frictional force** that arises between adjacent layers of fluid that are in relative motion.

Compilation of the ratio of shear viscosity to entropy density for various substances:

R. A. Lacey and A. Taranenko, PoS C FRNC2006, 021 (2006)

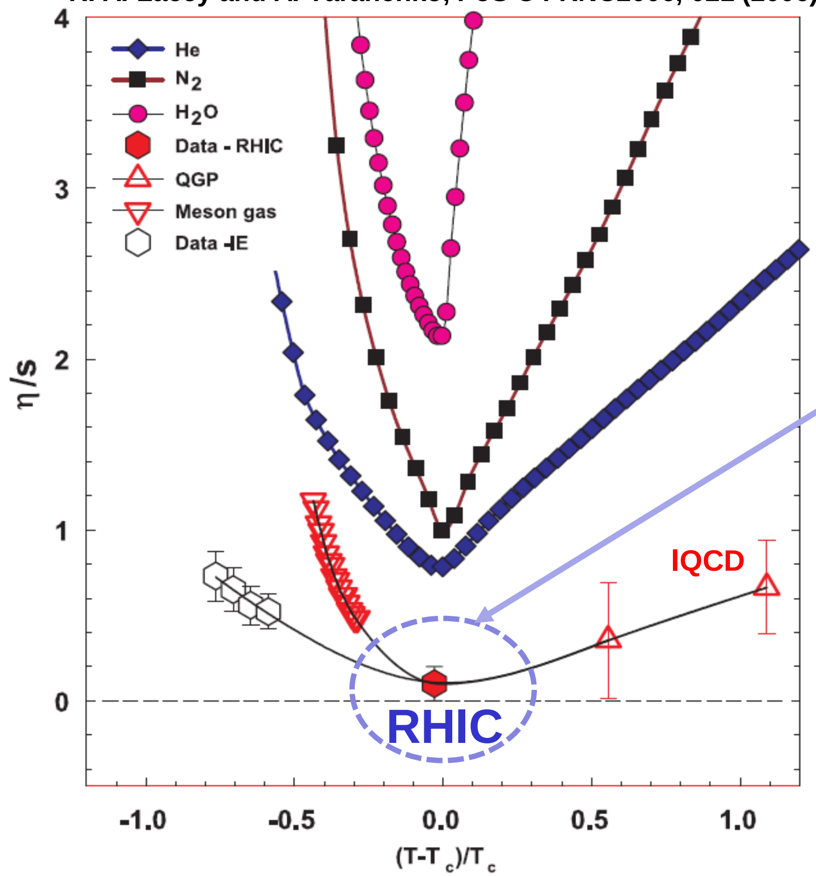

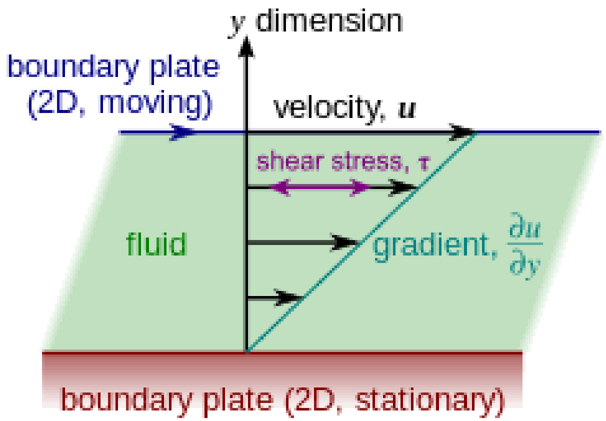

Exp. data + lQCD:
η/s near T_C is very small !

➔ QGP : close to an ideal liquid, not a gas of weakly interacting quarks and gluons

➔ QGP: strongly-interacting matter

pQCD: shear viscosity η

QCD: Pure Yang-Mills (only gluons)

LO (Leading order) perturbative QCD calculations:

$\eta/s > 0.5$ at T near T_C **'AMY': P.B. Arnold, G.D. Moore and L.G. Yaffe,, JHEP 11 (2000) 001)**

NLO (Next-to-leading order): **(J. Ghiglieri, G.D. Moore, D. Teaney, JHEP 1803 (2018) 179):**
"The next-to-leading order corrections are large and bring η/s down by more than a factor of 3 at physically relevant couplings.
The perturbative expansion is problematic even at T ~100 GeV"

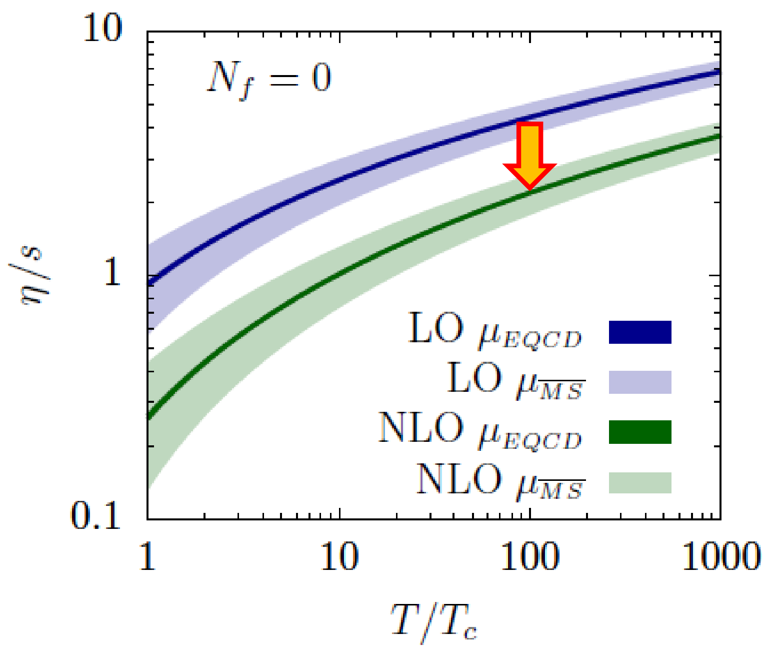

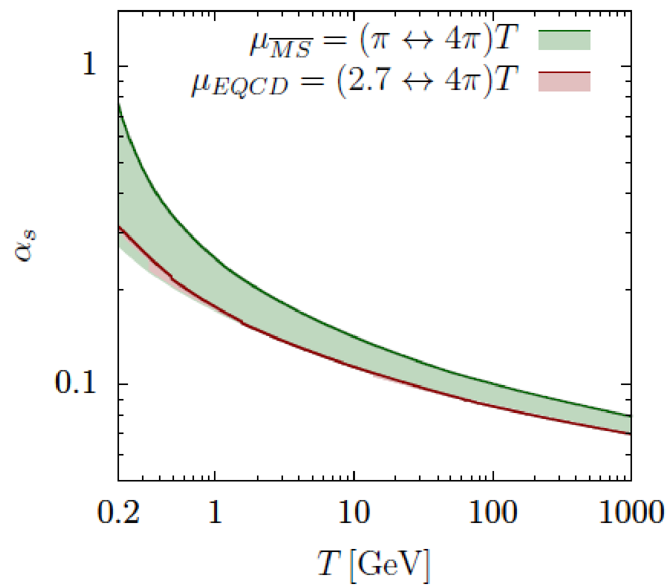

➔ from pQCD to effective models of QCD!

Transport coefficients: shear viscosity η

- **Relaxation Time Approximation**

$$\eta^{\mathrm{RTA}}(T,\mu_B) = \frac{1}{15T}\sum_{i=q,\bar{q},g}\int \frac{d^3p}{(2\pi)^3}\frac{\mathbf{p}^4}{E_i^2}\boxed{\tau_i(\mathbf{p},T,\mu_B)}\, d_i(1\pm f_i)f_i$$

$$1)\,\tau_i(\mathbf{p},T,\mu_B) = \frac{1}{\Gamma_i(\mathbf{p},T,\mu_B)}$$

$$2)\,\tau_i(T,\mu_B) = \frac{1}{2\gamma_i(T,\mu_B)},$$

η/s versus (T,μ_B)

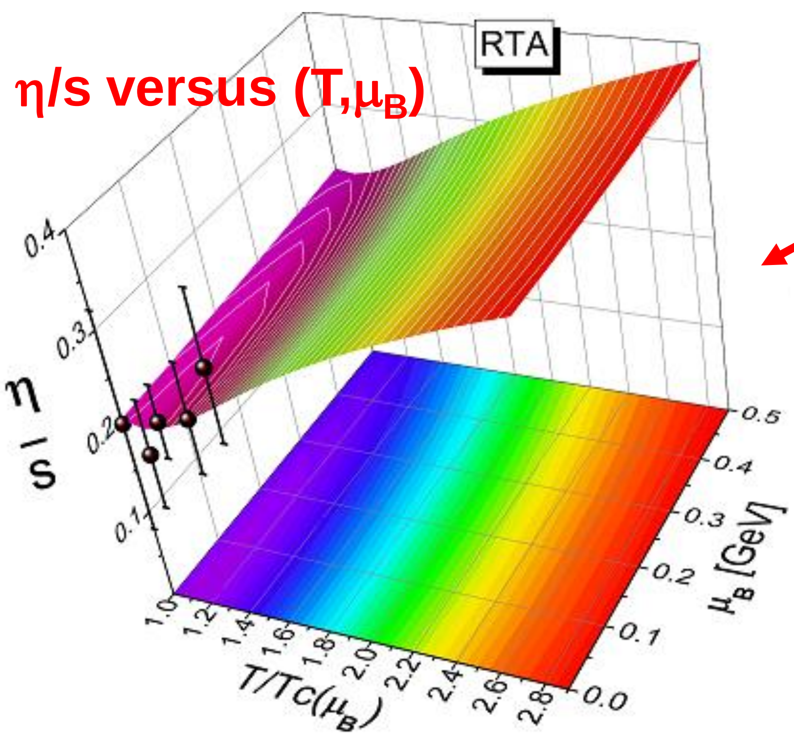

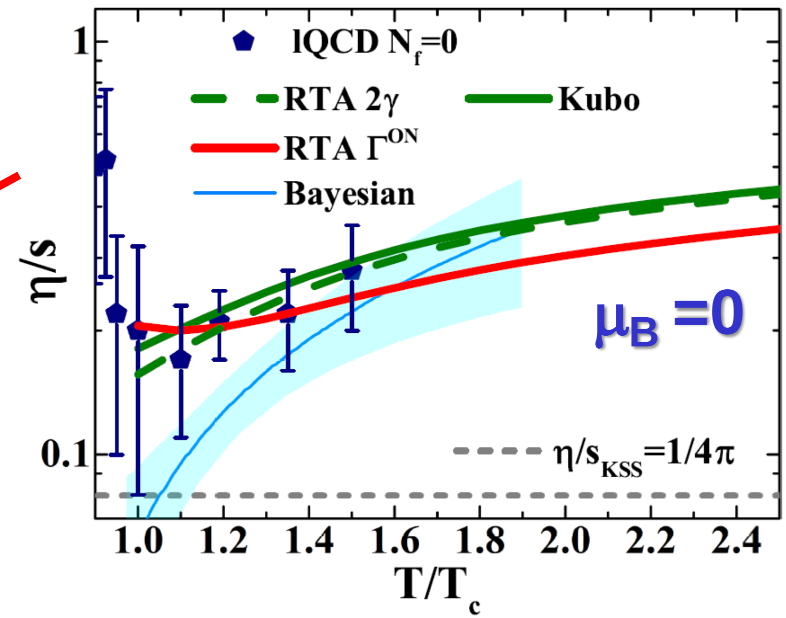

Hydro: Bayesian analysis, S. Bass et al. , NPA967 (2017) 67
Kovtun-Son-Starinets bound : $(\eta/s)_{KSS} = 1/(4\pi)$

- **Weak dependence of shear viscosity on μ_B**

Lattice QCD: N. Astrakhantsev et al, JHEP 1704 (2017) 101

P. Moreau et al., PRC100 (2019) 014911; O. Soloveva et al., PRC110 (2020) 045203

Transport coefficients: bulk viscosity ζ

➢ Relaxation Time Approximation

$$\zeta^{\mathrm{RTA}}(T,\mu_B) = \frac{1}{9T}\sum_{i=q,\bar{q},g}\int \frac{d^3p}{(2\pi)^3}\boxed{\tau_i(\mathbf{p},T,\mu_B)}$$

Relaxation times

$$\times\ \frac{d_i(1\pm f_i)f_i}{E_i^2}\left(\mathbf{p}^2 - 3c_s^2\left(E_i^2 - T^2\frac{dm_i^2}{dT^2}\right)\right)^2$$

From DQPM parametrization

Speed of sound

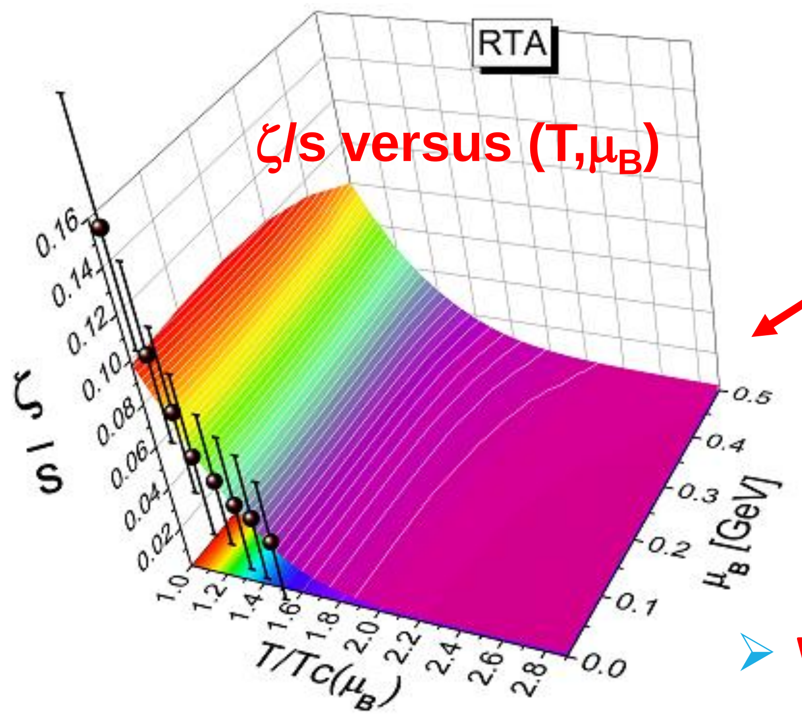

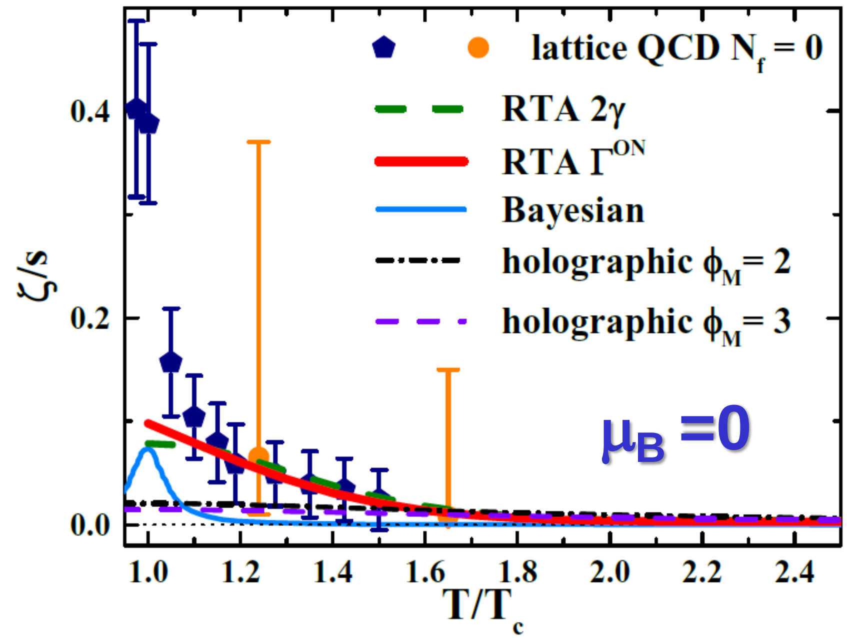

Lattice: Astrakhantsev et al, Phys.Rev. D98 (2018) 054515

➢ **Weak dependence of bulk viscosity on μ_B**

P. Moreau et al., PRC100 (2019) 014911; O. Soloveva et al., PRC110 (2020) 045203

Transport coefficients: electric conductivity σ_e/T

σ_0 → Probe of electric properties of the QGP

η/s versus (T,μ_B)

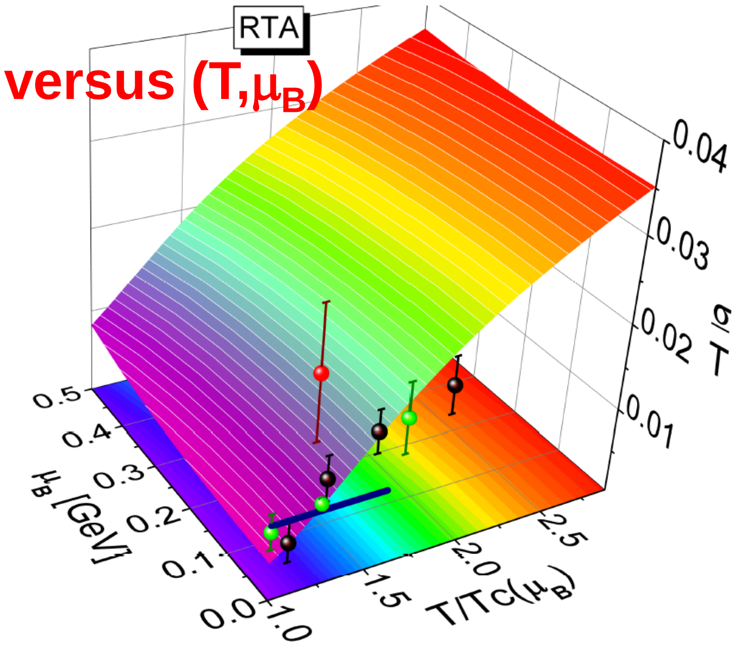

➢ **Relaxation Time Approximation**

$$\sigma_0^{\mathrm{RTA}}(T,\mu_B) = \frac{e^2}{3T}\sum_{i=q,\bar{q}} q_i^2 \int \frac{d^3p}{(2\pi)^3}\frac{\mathbf{p}^2}{E_i^2}$$

$$\times \boxed{\tau_i(\mathbf{p},T,\mu_B)}\, d_i(1-f_i)f_i$$

▪ **the QCD matter even at $T\sim T_c$ is a much better electric conductor than Cu or Ag (at room temperature) by a factor of 500 !**

Exp. observables – photon and dilepton spectra

❑ **Photon emission:** rates for $q_0 \to 0$ are related to electric conductivity σ_0

$$q_0 \left.\frac{dR}{d^4x\, d^3q}\right|_{q_0\to 0} = \frac{T}{4\pi^3}\sigma_0$$

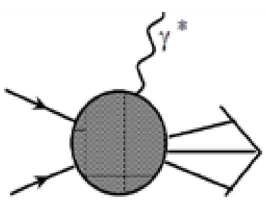

O. Soloveva et al., PRC110 (2020) 045203

Review: H. Berrehrah et al. Int.J.Mod.Phys. E25 (2016) 1642003

QGP:
in-equilibrium ➔ off-equilibrium

microscopic transport theory!

From weakly to strongly interacting systems

Properties of matter (on hadronic and partonic levels) **in heavy-ion collisions:**
QGP – strongly interacting system! Degrees of freedom – dressed partons!
Hadronic matter – in-medium effects – modification of hadron properties at finite T, μ_B (vector mesons, strange mesons)

Many-body theory:
Strong interaction ➔ **large width** = short life-time
➔ broad spectral function ➔ **quantum object**

- **How to describe the dynamics of broad strongly interacting quantum states in transport theory?**

- ❑ semi-classical BUU

first order gradient expansion of quantum Kadanoff-Baym equations

- ❑ **generalized transport equations based on Kadanoff-Baym dynamics**

Kbar* spectral function

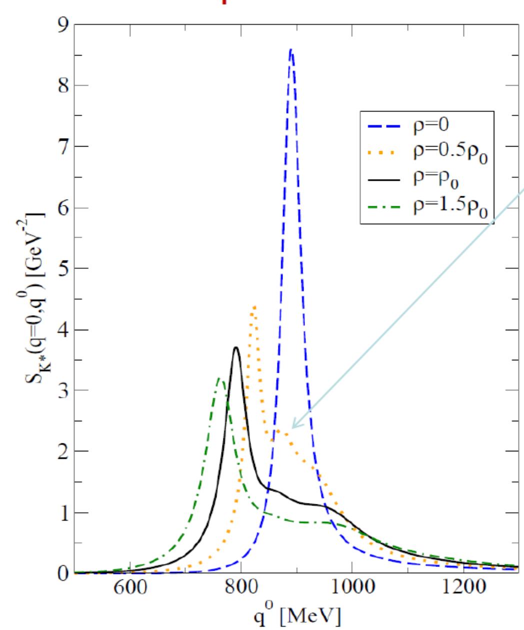

$\Lambda(1783)N^{-1}$ and $\Sigma(1830)N^{-1}$ exitations

Barcelona / Valencia group

Dynamical description of strongly interacting systems

- **Quantum field theory ➔**

Kadanoff-Baym dynamics **for resummed single-particle Green functions S**

$$\boxed{\hat{S}_{0x}^{-1}\, S_{xy}^{<} = \Sigma_{xz}^{ret} \odot S_{zy}^{<} + \Sigma_{xz}^{<} \odot S_{zy}^{adv}}$$

(1962)

Integration over the intermediate spacetime

Green functions $S^<$ / self-energies Σ:

$$iS_{xy}^{<} = \eta \langle \{\Phi^{+}(y)\Phi(x)\}\rangle$$

$$iS_{xy}^{>} = \langle \{\Phi(y)\Phi^{+}(x)\}\rangle$$

$$iS_{xy}^{c} = \langle T^{c}\{\Phi(x)\Phi^{+}(y)\}\rangle \quad -causal$$

$$iS_{xy}^{a} = \langle T^{a}\{\Phi(x)\Phi^{+}(y)\}\rangle \quad -anticausal$$

$$S_{xy}^{ret} = S_{xy}^{c} - S_{xy}^{<} = S_{xy}^{>} - S_{xy}^{a} \quad -retarded$$

$$S_{xy}^{adv} = S_{xy}^{c} - S_{xy}^{>} = S_{xy}^{<} - S_{xy}^{a} \quad -advanced$$

$$\hat{S}_{0x}^{-1} \equiv -(\partial_x^{\mu}\partial_{\mu}^{x} + M_0^2)$$

$$\eta = \pm 1 (bosons\, /\, fermions)$$

$$T^{a}(T^{c}) - (anti-)time-ordering\ operator$$

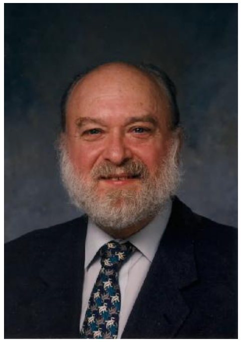

Leo Kadanoff

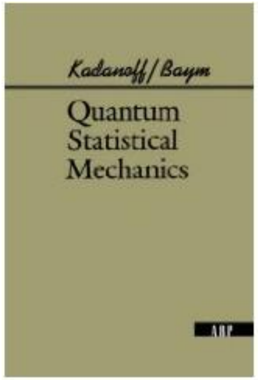

Gordon Baym

From Kadanoff-Baym equations to generalized transport equations

After the first order gradient expansion of the Wigner transformed Kadanoff-Baym equations and separation into the real and imaginary parts one gets:

Generalized transport equations (GTE):

drift term — Vlasov term — backflow term — collision term = ‚gain' - ‚loss' term

$$\diamond\{P^2 - M_0^2 - Re\Sigma^{ret}_{XP}\}\{S^<_{XP}\} - \boxed{\diamond\{\Sigma^<_{XP}\}\{ReS^{ret}_{XP}\}} = \frac{i}{2}\left[\Sigma^>_{XP}S^<_{XP} - \Sigma^<_{XP}S^>_{XP}\right]$$

Backflow term incorporates the off-shell behavior in the particle propagation

! vanishes in the quasiparticle limit $A_{XP} \rightarrow \delta(p^2-M^2)$

- GTE: Propagation of the Green's function $iS^<_{XP}=A_{XP}N_{XP}$, which carries information not only on the number of particles (N_{XP}), but also on their properties, interactions and correlations (via A_{XP})

- Spectral function:

$$A_{XP} = \frac{\Gamma_{XP}}{(P^2 - M_0^2 - Re\Sigma^{ret}_{XP})^2 + \Gamma^2_{XP}/4}$$

$\Gamma_{XP} = -Im\,\Sigma^{ret}_{XP} = 2\,p_0\Gamma$ – ‚width' of spectral function

= reaction rate of particle (at space-time position X)

4-dimentional generalizaton of the Poisson-bracket:

$$\diamond\{F_1\}\{F_2\} := \frac{1}{2}\left(\frac{\partial F_1}{\partial X_\mu}\frac{\partial F_2}{\partial P^\mu} - \frac{\partial F_1}{\partial P_\mu}\frac{\partial F_2}{\partial X^\mu}\right)$$

- Life time $\tau = \frac{\hbar c}{\Gamma}$

W. Cassing , S. Juchem, NPA 665 (2000) 377; 672 (2000) 417; 677 (2000) 445

General testparticle off-shell equations of motion

W. Cassing , S. Juchem, NPA 665 (2000) 377; 672 (2000) 417; 677 (2000) 445

- Employ testparticle Ansatz for the real valued quantity $i\,S^<_{XP}$

$$F_{XP} = A_{XP} N_{XP} = i\,S^<_{XP} \sim \sum_{i=1}^{N} \delta^{(3)}(\vec{X} - \vec{X}_i(t))\ \delta^{(3)}(\vec{P} - \vec{P}_i(t))\ \delta(P_0 - \epsilon_i(t))$$

insert in generalized transport equations and determine equations of motion !

➔ **General testparticle Cassing's off-shell equations of motion for the time-like particles:**

$$\frac{d\vec{X}_i}{dt} = \frac{1}{1 - C_{(i)}} \frac{1}{2\epsilon_i} \left[2\,\vec{P}_i + \vec{\nabla}_{P_i} Re\Sigma^{ret}_{(i)} + \frac{\epsilon_i^2 - \vec{P}_i^2 - M_0^2 - Re\Sigma^{ret}_{(i)}}{\Gamma_{(i)}} \vec{\nabla}_{P_i} \Gamma_{(i)} \right],$$

$$\frac{d\vec{P}_i}{dt} = -\frac{1}{1 - C_{(i)}} \frac{1}{2\epsilon_i} \left[\vec{\nabla}_{X_i} Re\Sigma^{ret}_i + \frac{\epsilon_i^2 - \vec{P}_i^2 - M_0^2 - Re\Sigma^{ret}_{(i)}}{\Gamma_{(i)}} \vec{\nabla}_{X_i} \Gamma_{(i)} \right],$$

$$\frac{d\epsilon_i}{dt} = \frac{1}{1 - C_{(i)}} \frac{1}{2\epsilon_i} \left[\frac{\partial Re\Sigma^{ret}_{(i)}}{\partial t} + \frac{\epsilon_i^2 - \vec{P}_i^2 - M_0^2 - Re\Sigma^{ret}_{(i)}}{\Gamma_{(i)}} \frac{\partial \Gamma_{(i)}}{\partial t} \right],$$

with $F_{(i)} \equiv F(t, \vec{X}_i(t), \vec{P}_i(t), \epsilon_i(t))$

$$C_{(i)} = \frac{1}{2\epsilon_i} \left[\frac{\partial}{\partial \epsilon_i} Re\Sigma^{ret}_{(i)} + \frac{\epsilon_i^2 - \vec{P}_i^2 - M_0^2 - Re\Sigma^{ret}_{(i)}}{\Gamma_{(i)}} \frac{\partial}{\partial \epsilon_i} \Gamma_{(i)} \right]$$

Collision term in off-shell transport models

Collision term for reaction 1+2->3+4:

$$I_{coll}(X,\vec{P},M^2) = Tr_2 Tr_3 Tr_4 A(X,\vec{P},M^2) A(X,\vec{P}_2,M_2^2) A(X,\vec{P}_3,M_3^2) A(X,\vec{P}_4,M_4^2)$$

$$|G((\vec{P},M^2)+(\vec{P}_2,M_2^2) \rightarrow (\vec{P}_3,M_3^2)+(\vec{P}_4,M_4^2))|^2_{\mathcal{A},\mathcal{S}} \; \delta^{(4)}(P+P_2-P_3-P_4)$$

$$[\, N_{X\vec{P}_3M_3^2}\, N_{X\vec{P}_4M_4^2}\, \bar{f}_{X\vec{P}M^2}\, \bar{f}_{X\vec{P}_2M_2^2} \;-\; N_{X\vec{P}M^2}\, N_{X\vec{P}_2M_2^2}\, \bar{f}_{X\vec{P}_3M_3^2}\, \bar{f}_{X\vec{P}_4M_4^2} \,]$$

‚gain‘ term ‚loss‘ term

with $\bar{f}_{X\vec{P}M^2} = 1 + \eta\, N_{X\vec{P}M^2}$ and $\eta = \pm 1$ for bosons/fermions, respectively.

The trace over particles 2,3,4 reads explicitly

for fermions

$$Tr_2 = \sum_{\sigma_2,\tau_2} \frac{1}{(2\pi)^4} \int d^3P_2 \frac{dM_2^2}{2\sqrt{\vec{P}_2^2 + M_2^2}}$$

for bosons

$$Tr_2 = \sum_{\sigma_2,\tau_2} \frac{1}{(2\pi)^4} \int d^3P_2 \frac{dP_{0,2}^2}{2}$$

additional integration

The transport approach and the particle spectral functions are fully determined once the in-medium transition amplitudes G are known in their off-shell dependence!

Parton-Hadron-String-Dynamics (PHSD)

PHSD is a **non-equilibrium microscopic transport approach** for the description of **strongly-interacting hadronic and partonic matter** created in heavy-ion collisions

Dynamics: based on the solution of **generalized off-shell transport equations** derived from Kadanoff-Baym many-body theory

Initial A+A collision

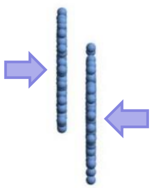

Partonic phase

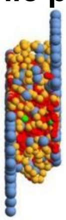

Hadronization

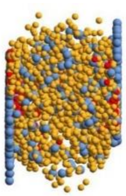

Hadronic phase

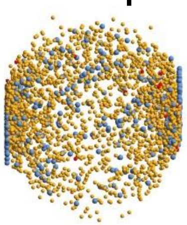

- **Initial A+A collisions** :
  N+N → string formation → decay to pre-hadrons + leading hadrons

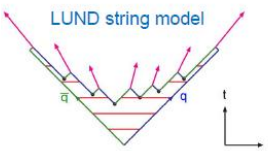

- **Formation of QGP stage** if local $\varepsilon > \varepsilon_{critical}$:
  dissolution of pre-hadrons → partons

- **Partonic phase - QGP:**
  QGP is described by the Dynamical QuasiParticle Model (DQPM) matched to reproduce lattice QCD EoS for finite T and μ_B (crossover)

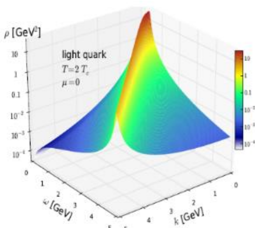

- Degrees-of-freedom: strongly interacting quasiparticles: massive quarks and gluons (g,q,q_{bar}) with sizeable collisional widths in a self-generated mean-field potential

- Interactions: (quasi-)elastic and inelastic collisions of partons

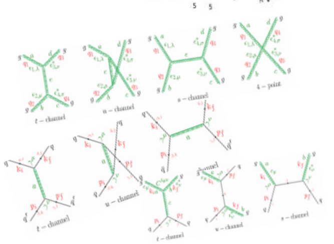

- **Hadronization** to colorless **off-shell mesons and baryons**:
  Strict 4-momentum and quantum number conservation

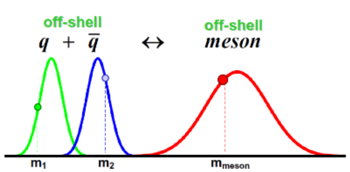

- **Hadronic phase: hadron-hadron interactions – off-shell HSD**

W. Cassing, E. Bratkovskaya, PRC 78 (2008) 034919; NPA831 (2009) 215; W. Cassing, EPJ ST 168 (2009) 3

Traces of the QGP in observables in high energy heavy-ion collisions

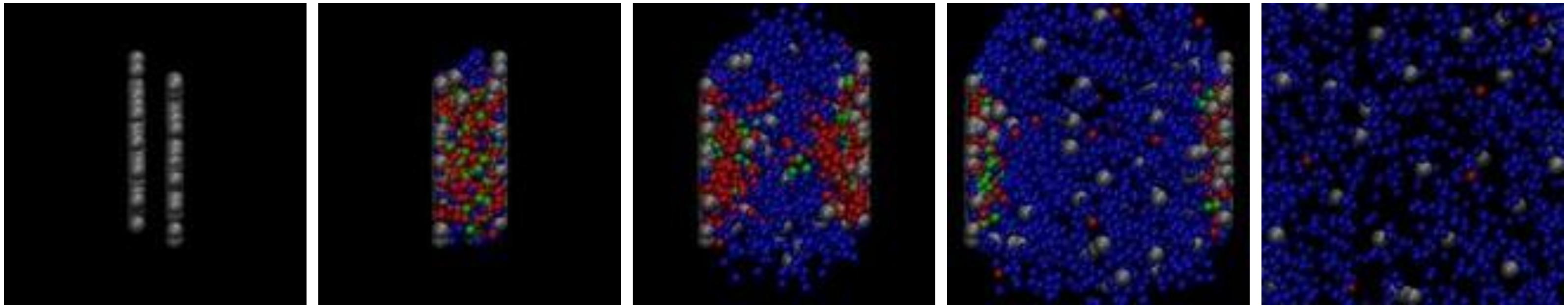

Stages of a collision in PHSD

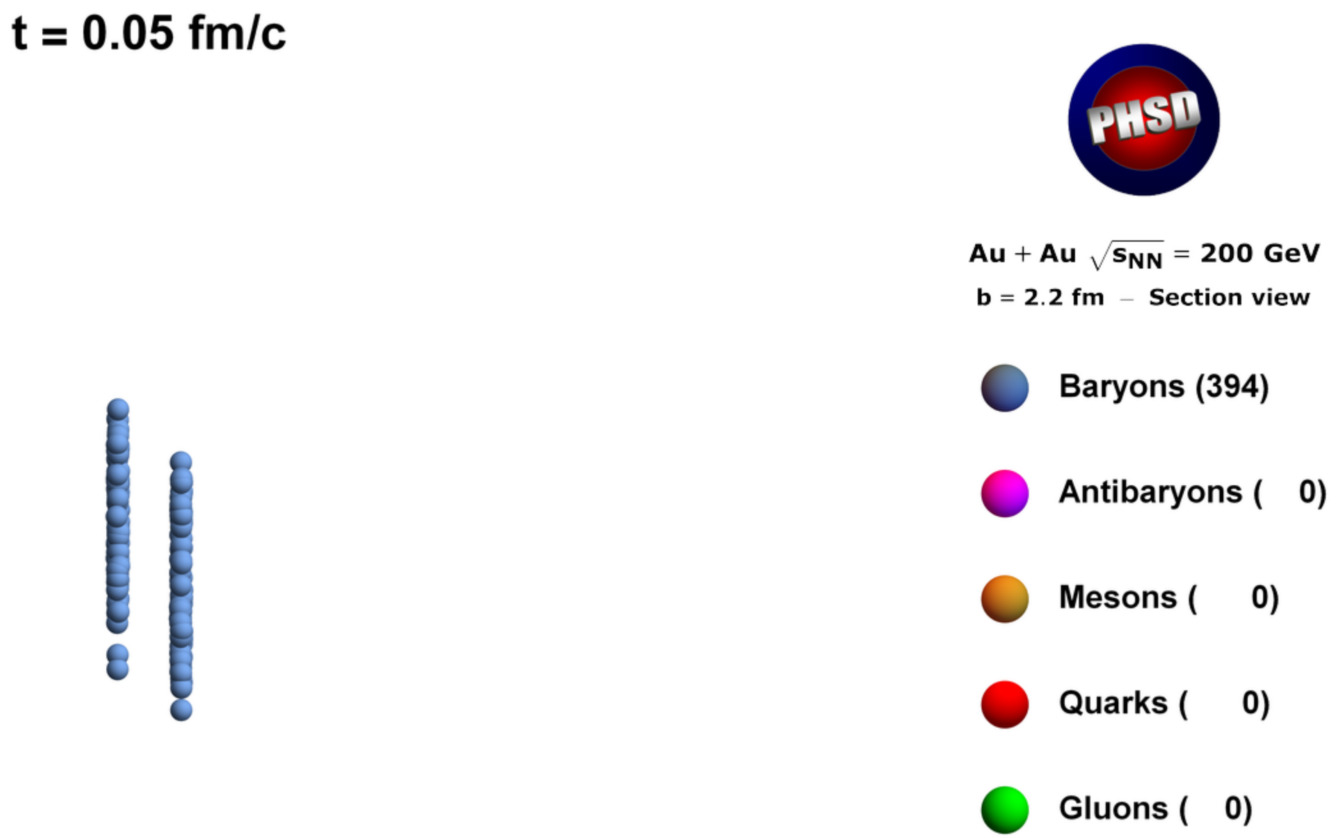

P.Moreau

Stages of a collision in PHSD

t = 1.6512 fm/c

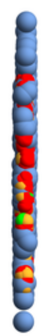

Au + Au $\sqrt{s_{NN}}$ = 200 GeV
b = 2.2 fm – Section view

- Baryons (394)
- Antibaryons (0)
- Mesons (1523)
- Quarks (4553)
- Gluons (368)

P.Moreau

Stages of a collision in PHSD

t = 3.91921 fm/c

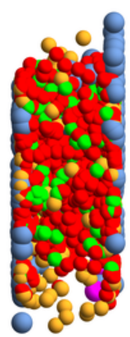

Au + Au $\sqrt{s_{NN}}$ = 200 GeV

b = 2.2 fm – Section view

Baryons (426)

Antibaryons (29)

Mesons (1189)

Quarks (4459)

Gluons (783)

P.Moreau

Stages of a collision in PHSD

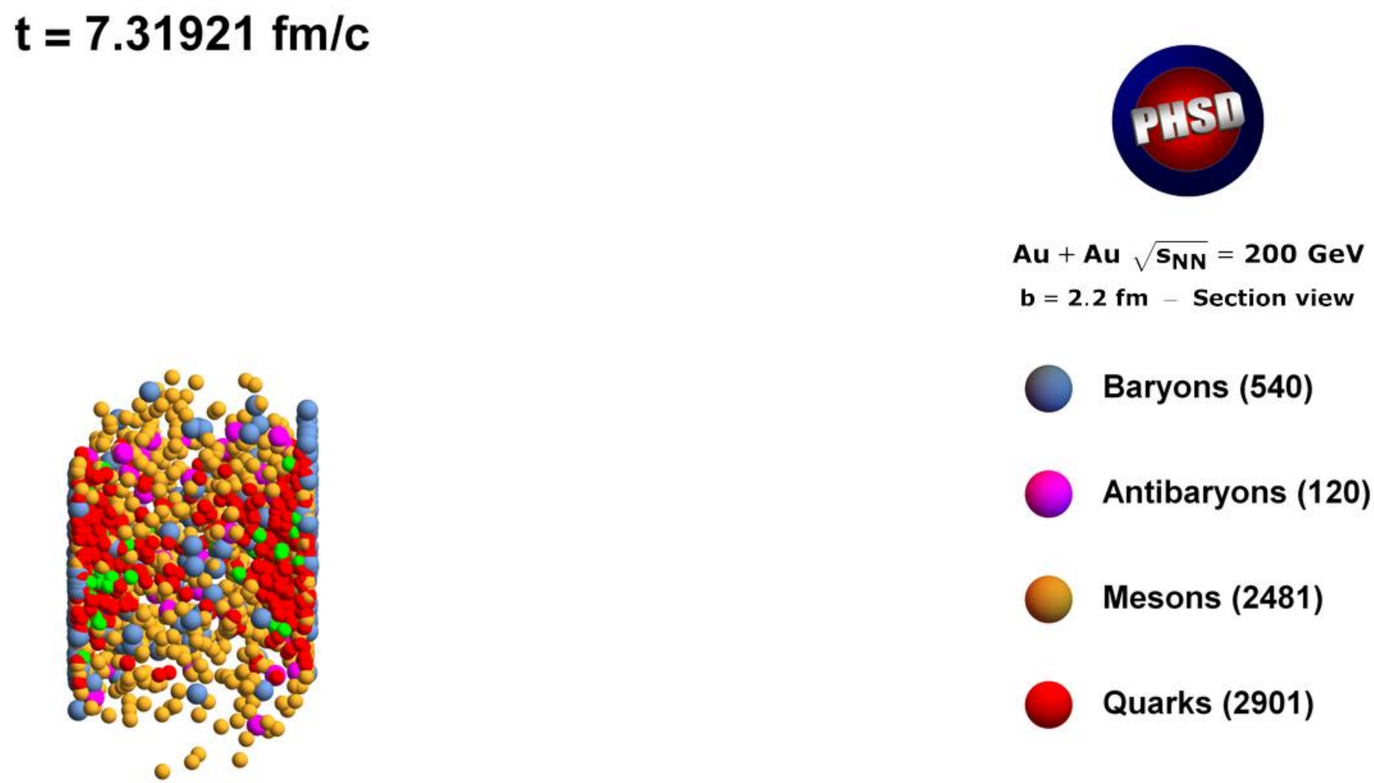

P.Moreau

Stages of a collision in PHSD

t = 12.0192 fm/c

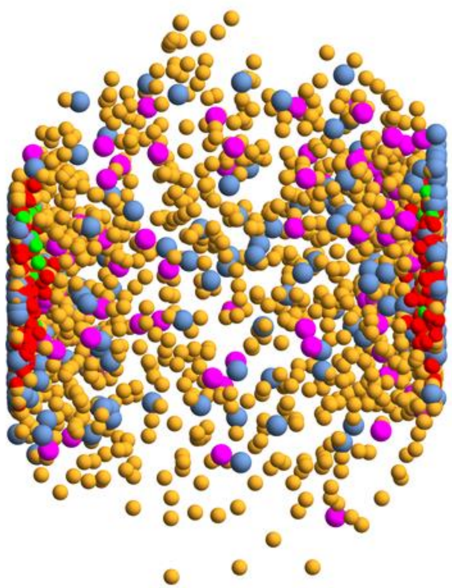

Au + Au $\sqrt{s_{NN}}$ = 200 GeV

b = 2.2 fm – Section view

- Baryons (626)
- Antibaryons (202)
- Mesons (3357)
- Quarks (1835)
- Gluons (269)

P.Moreau

Stages of a collision in PHSD

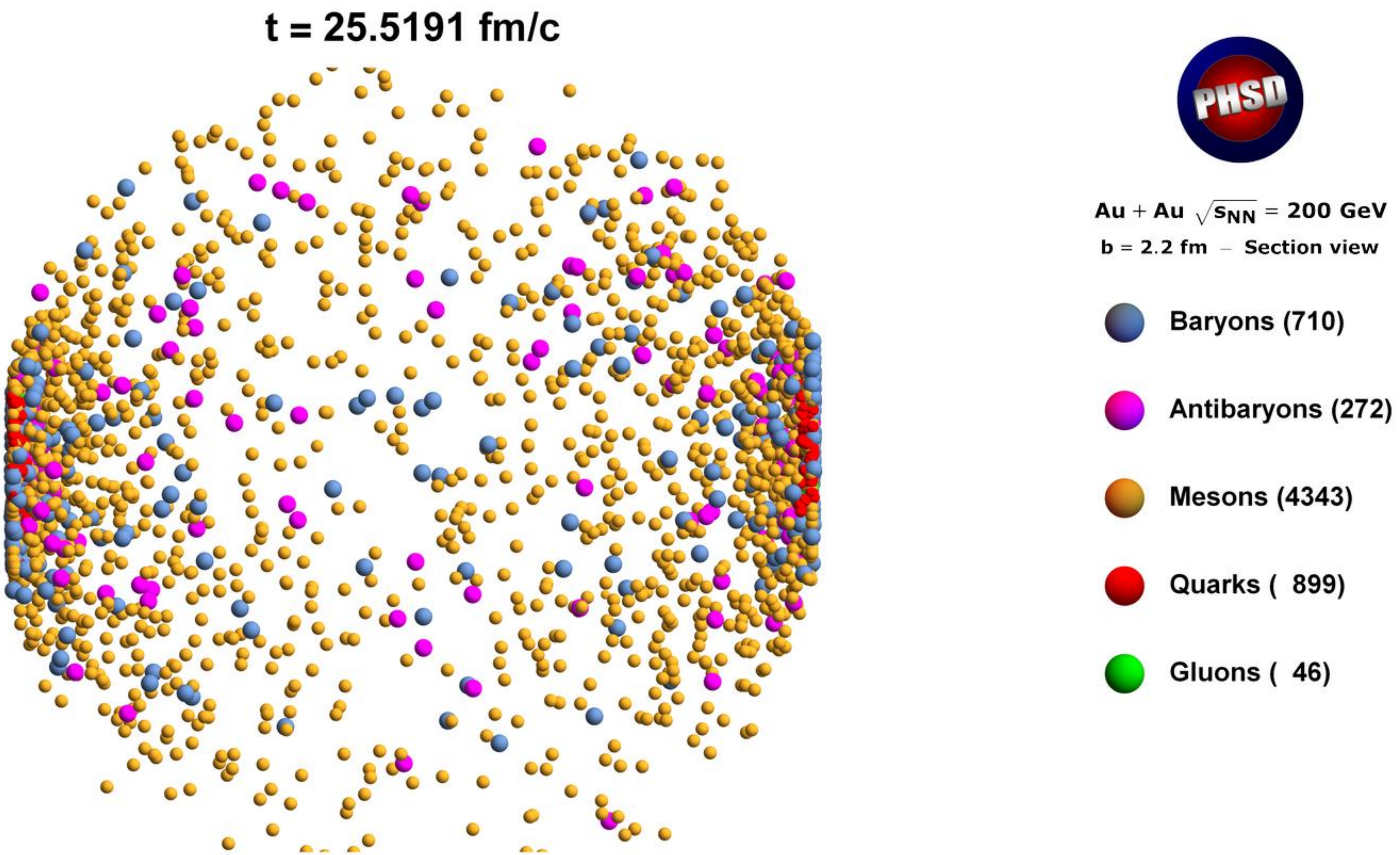

P.Moreau

Partonic energy fraction in central A+A

Time evolution of the partonic energy fraction vs energy

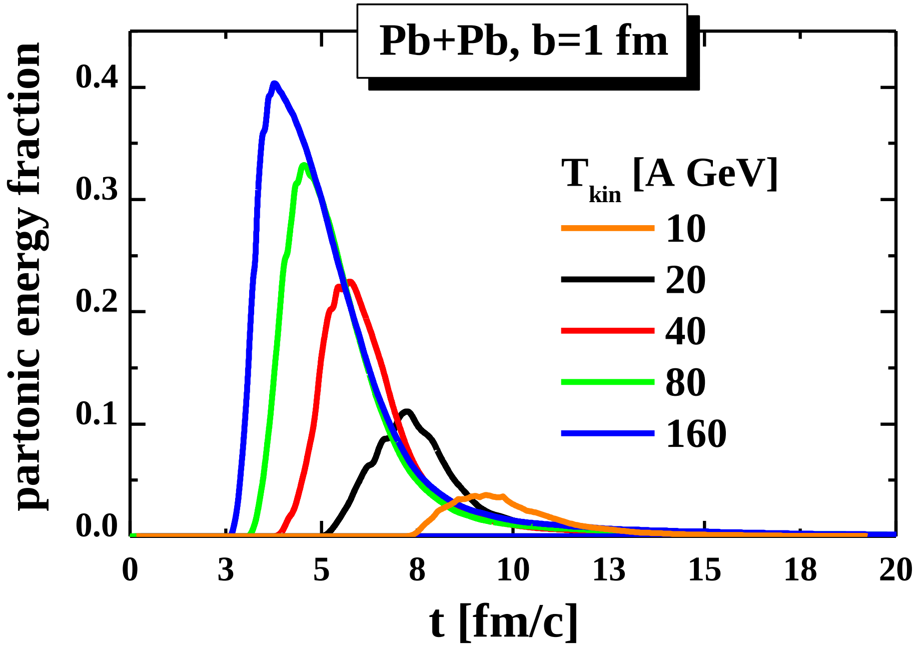

Au+Au, midrapidity

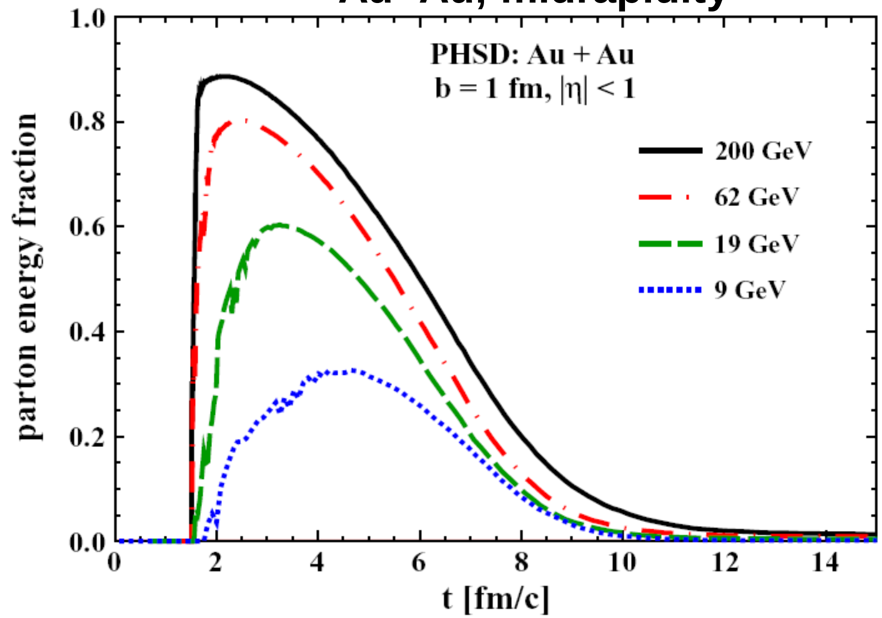

- Strong increase of partonic phase with energy from AGS to RHIC

- SPS: Pb+Pb, 160 A GeV: only about 40% of the converted energy goes to partons; the rest is contained in the large hadronic corona and leading partons
- RHIC: Au+Au, 21.3 A TeV: up to 90% - QGP

W. Cassing & E. Bratkovskaya, NPA 831 (2009) 215
V. Konchakovski et al., Phys. Rev. C 85 (2012) 011902

Time evolution of energy density

PHSD: 1 event Au+Au, 200 GeV, b = 2 fm

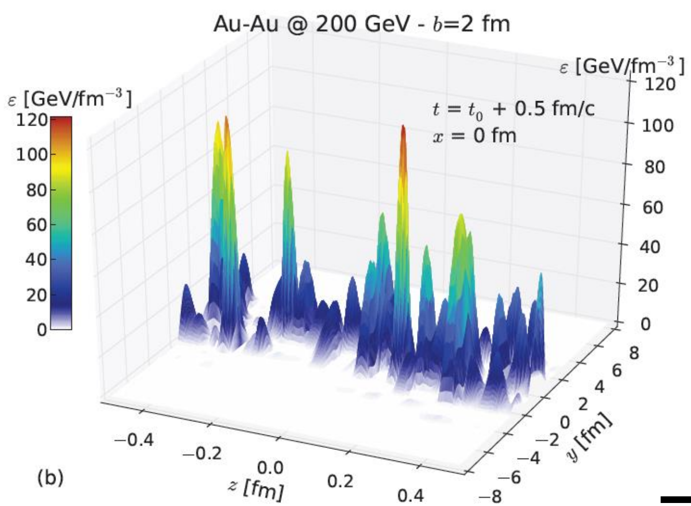

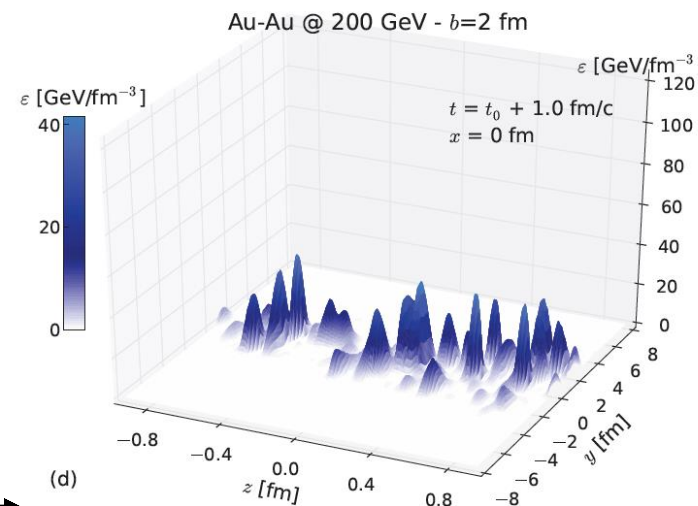

ε(x=0,y,z)

time

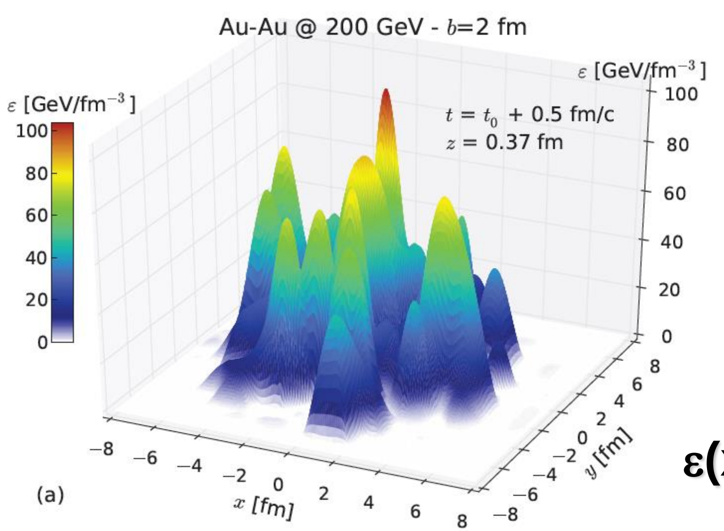

ε(x,y,z=0)

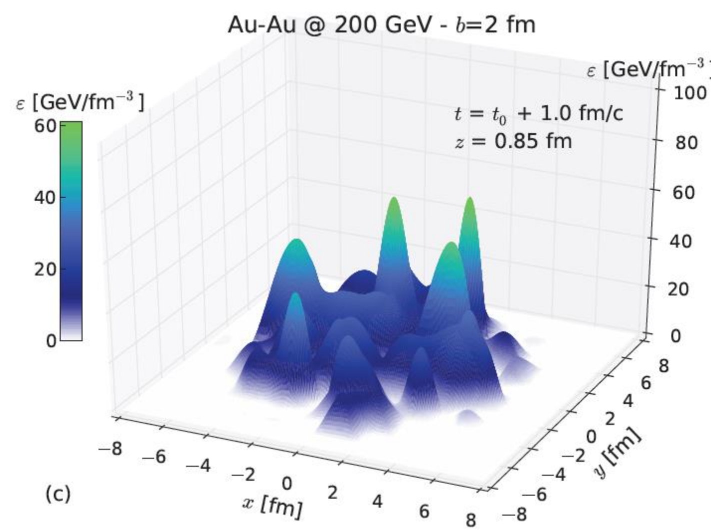

ΔV: $\Delta x=\Delta y$=1fm, $\Delta z=1/\gamma$ fm

R. Marty et al., PRC 92 (2015) 015201

Transverse mass spectra from SPS to RHIC

Central Pb + Pb at SPS energies

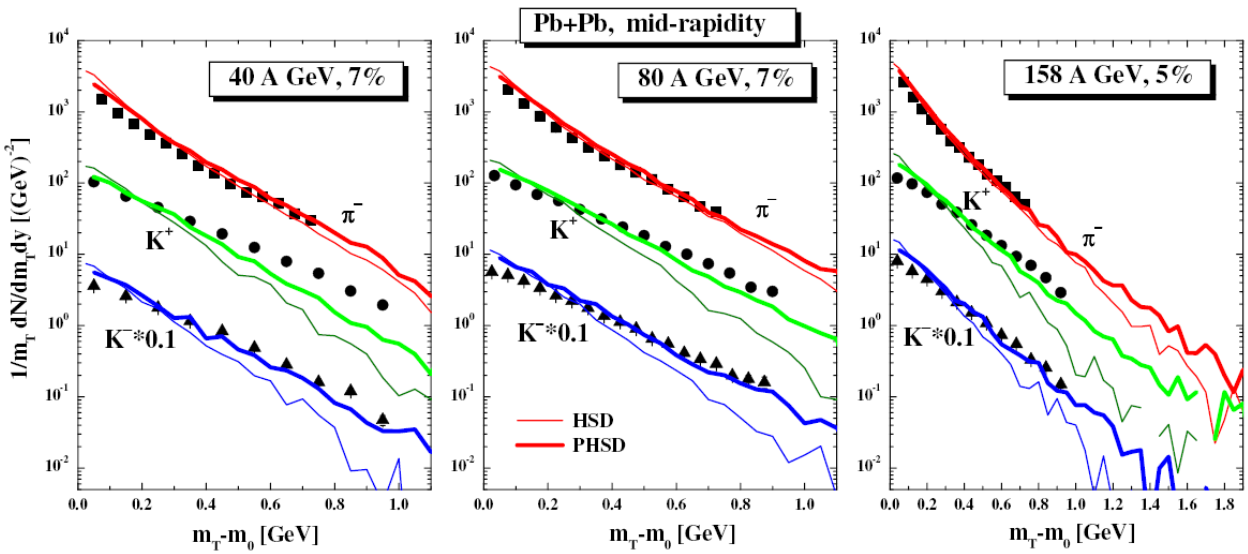

Central Au+Au at RHIC

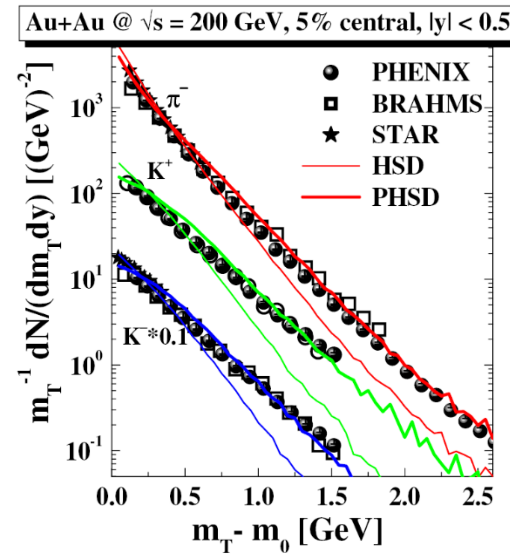

- PHSD gives harder m_T spectra and works better than HSD (without QGP) at high energies – RHIC, SPS (and top FAIR, NICA)
- however, at low SPS (and low FAIR, NICA) energies the effect of the partonic phase decreases due to the decrease of the partonic fraction

W. Cassing & E. Bratkovskaya, NPA 831 (2009) 215
E. Bratkovskaya, W. Cassing, V. Konchakovski, O. Linnyk, NPA856 (2011) 162

Anisotropy coefficients v_n

Non central Au+Au collisions :

- **interaction between constituents leads to a pressure gradient → spatial asymmetry is converted to an asymmetry in momentum space → collective flow**

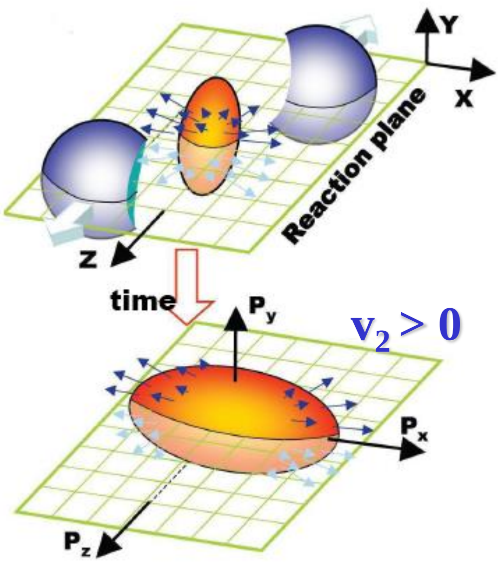

$$\frac{dN}{d\varphi} \propto \left(1 + 2\sum_{n=1}^{+\infty} v_n \cos\left[n(\varphi - \psi_n)\right]\right)$$

$$v_n = \left\langle \cos n\left(\varphi - \psi_n\right)\right\rangle, \quad n = 1,2,3..,$$

$$v_1 = \left\langle \frac{p_x}{p_T} \right\rangle, \quad v_2 = \left\langle \frac{p_x^2 - p_y^2}{p_x^2 + p_y^2} \right\rangle$$

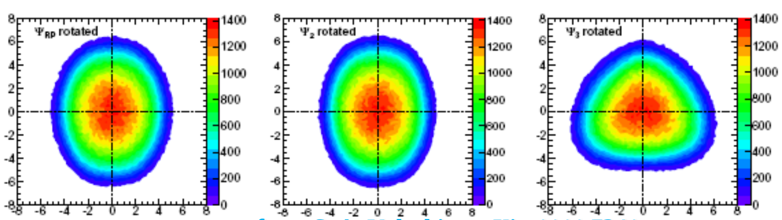

from S. A. Voloshin, arXiv:1111.7241

v_1: directed flow

v_2: elliptic flow

v_3: triangular flow

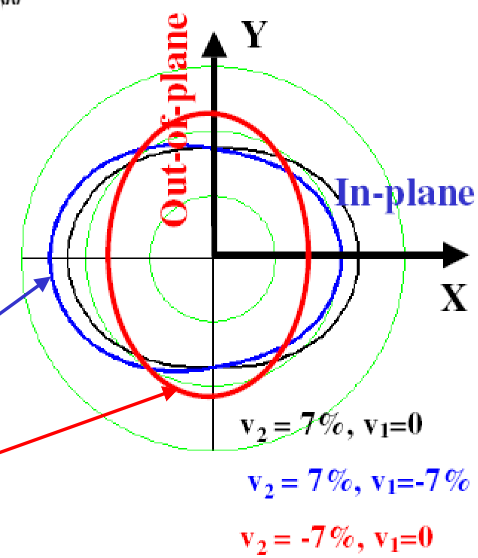

$v_2 > 0$ indicates in-plane emission of particles

$v_2 < 0$ corresponds to a squeeze-out perpendicular to the reaction plane (out-of-plane emission)

Hydrodynamic models: elliptic flow v_2

Comparison between hydro simulations and experimental data for the elliptic flow

Ideal hydrodynamic → **Viscous hydrodynamics**

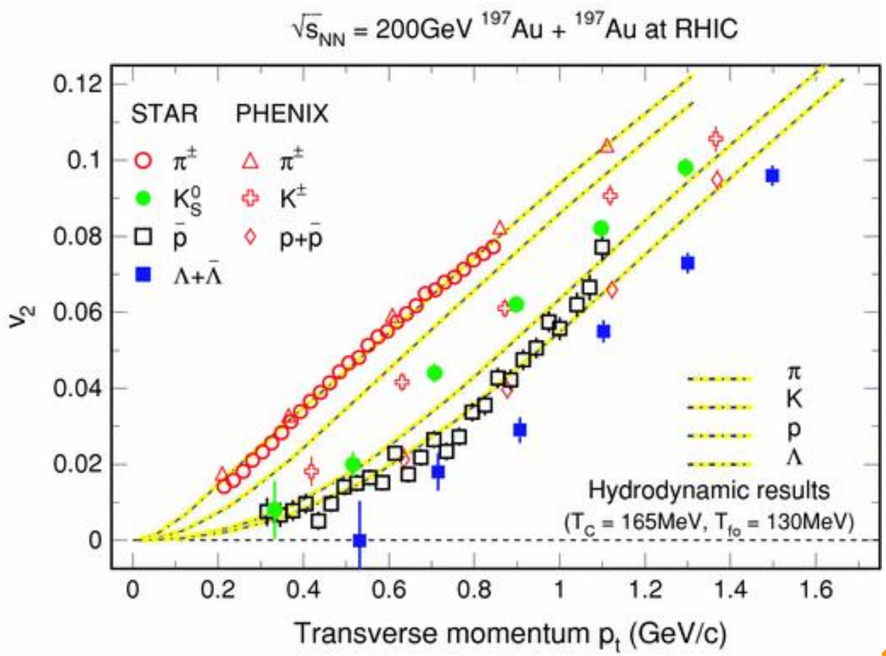

Heinz:2001

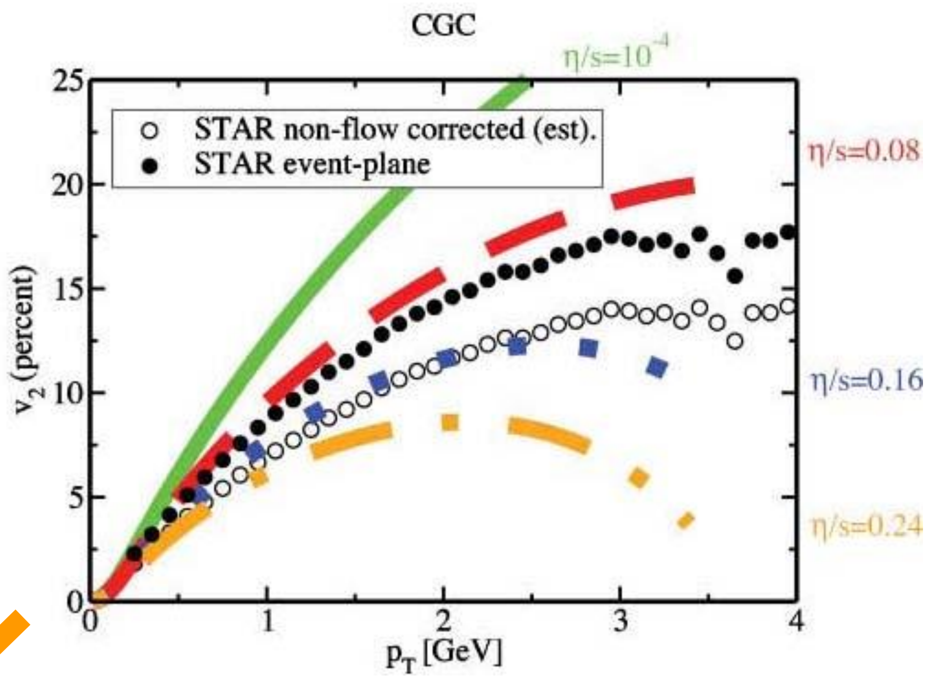

Luzum,Romatschke:2008

Ideal hydro: **reproduces exp. data at low p_T , overestimates v_2 at p_T > 1.2 GeV/c**

➔ Viscosity of QGP has to be accounted for ➔ viscous hydro

Elliptic flow v_2 is sensitive to η/s

Transport model PHSD: elliptic flow v_2

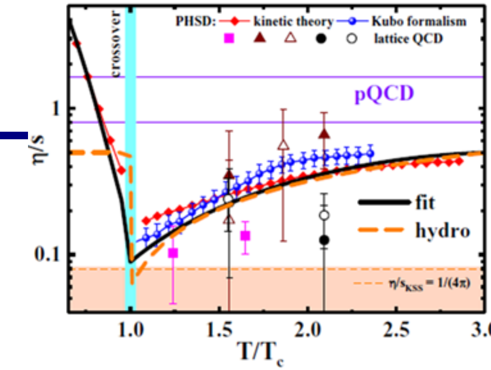

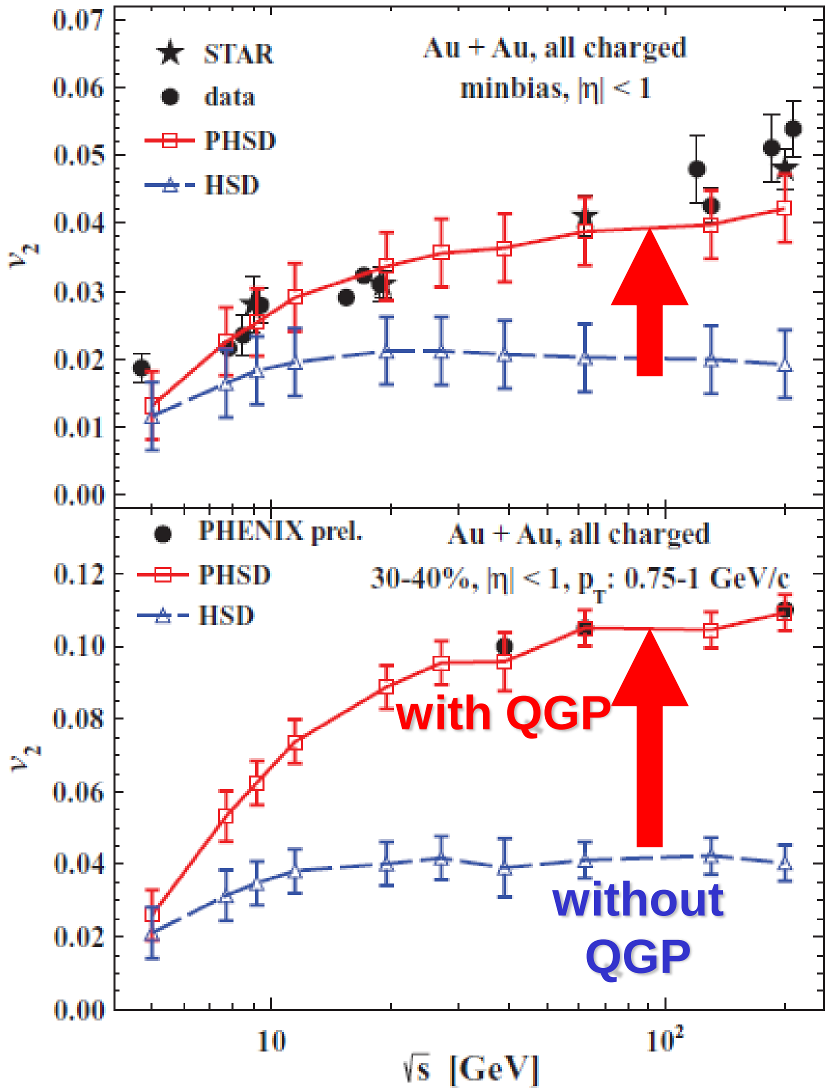

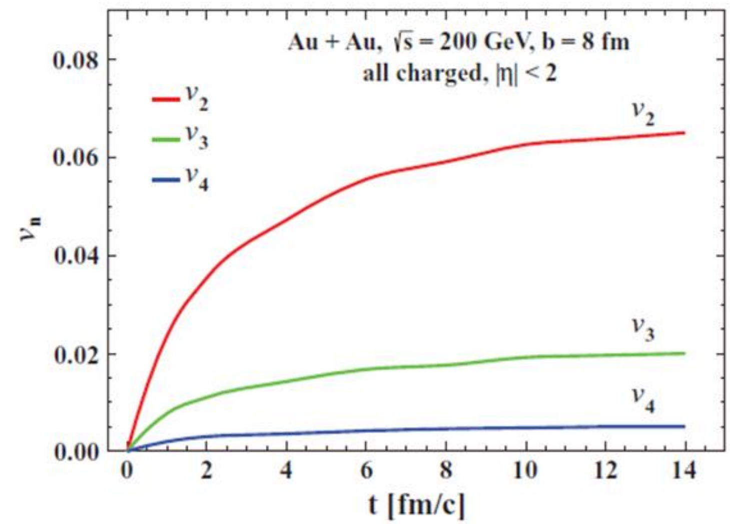

- v_2 in PHSD is larger than in HSD due to the repulsive scalar mean-field potential $U_s(\rho)$ for partons
- v_2 grows with bombarding energy due to the increase of the parton fraction

V. Konchakovski, E. Bratkovskaya, W. Cassing, V. Toneev, V. Voronyuk, Phys. Rev. C 85 (2012) 011902

V_n (n=2,3,4,5) of charged particles from PHSD at LHC

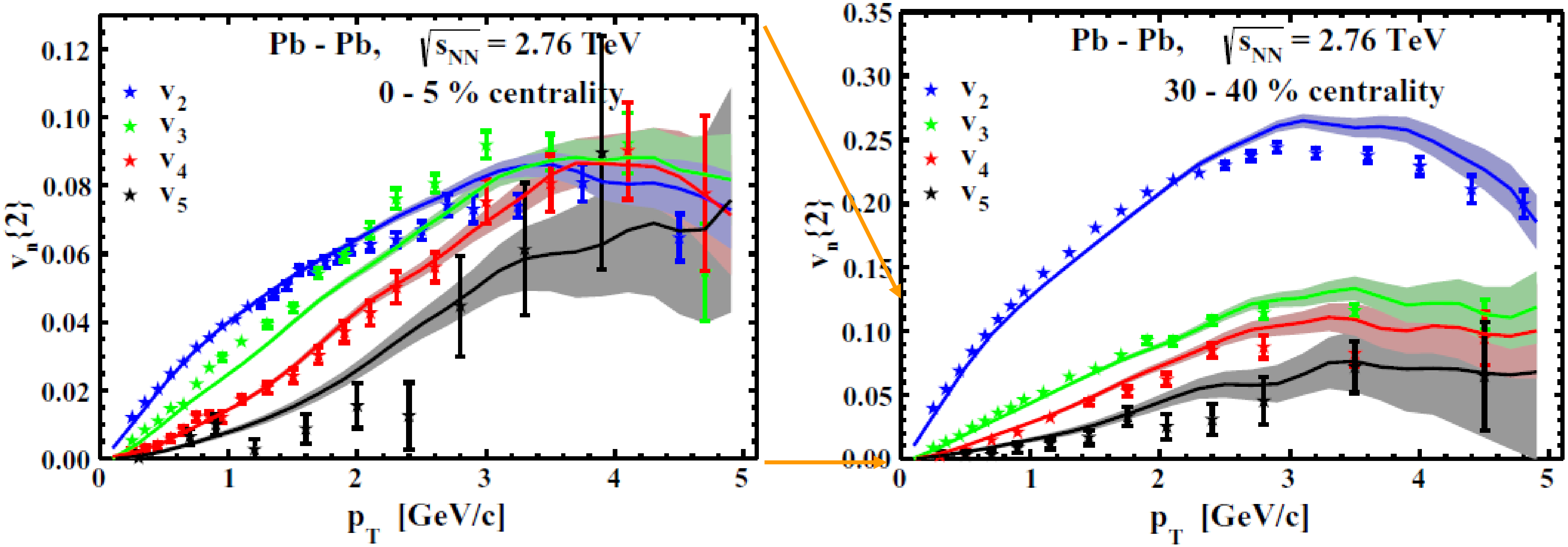

- PHSD: increase of v_n (n=2,3,4,5) with p_T
- v_2 increases with decreasing centrality
- v_n (n=3,4,5) show weak centrality dependence

symbols – ALICE
PRL 107 (2011) 032301
lines – PHSD (e-by-e)

v_n (n=3,4,5) develops by interactions in the QGP and in the final hadronic phase

V. Konchakovski, W. Cassing, V. Toneev, J. Phys. G: Nucl. Part. Phys 42 (2015) 055106

Traces of the QGP at finite μ_q in observables in high energy heavy-ion collisions

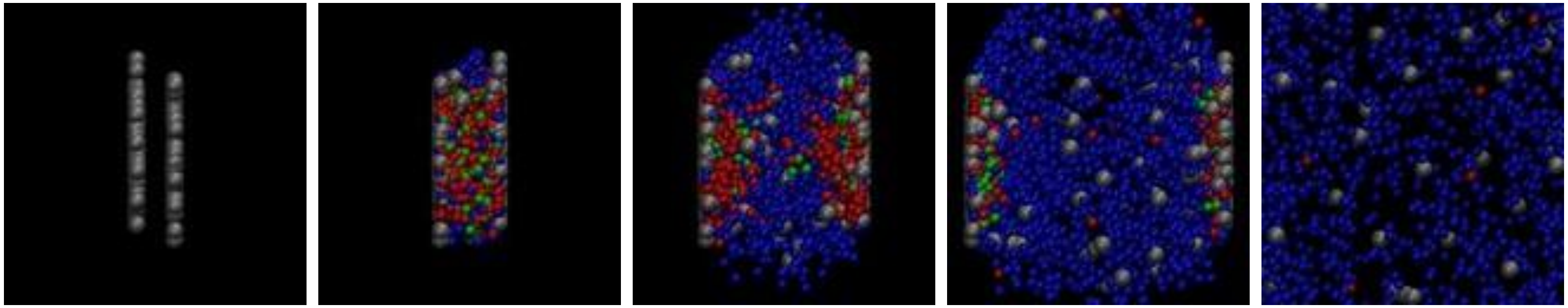

Extraction of (T, μ_B) in PHSD

- **For each cell in PHSD :**
  In order to extract (T, μ_B) use lQCD relations (up to 4th order) - Taylor series :

(1)
lQCD

$$\begin{cases} \dfrac{n_B}{T^3} \approx \chi_2^B(T)\left(\dfrac{\mu_B}{T}\right) + \cdots \\[2ex] \Delta\epsilon/T^4 \approx \dfrac{1}{2}\left(T\dfrac{\partial\chi_2^B(T)}{\partial T} + 3\chi_2^B(T)\right)\left(\dfrac{\mu_B}{T}\right)^2 + \cdots \end{cases}$$

*** Use baryon number susceptibilities χ_n from lQCD**

➔ **obtain (T, μ_B) by solving the system of coupled equations using ε^{PHSD} and n_B^{PHSD}**

*** Done by the Newton-Raphson method**

$e(x, y, z = 0)$

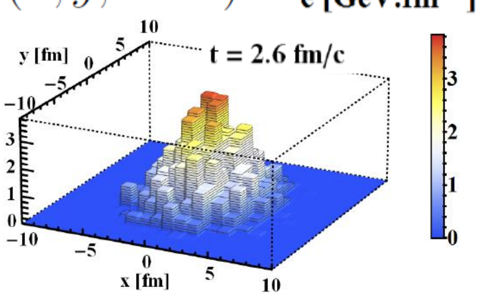

Au+Au, 200 GeV, b=6 fm

Input:

ε^{PHSD} and n_B^{PHSD}

(1)

lQCD

Output:

T, μ_B

P. Moreau et al., PRC100 (2019) 014911

Illustration for a HIC ($\sqrt{s_{NN}} = 19.6$ GeV)

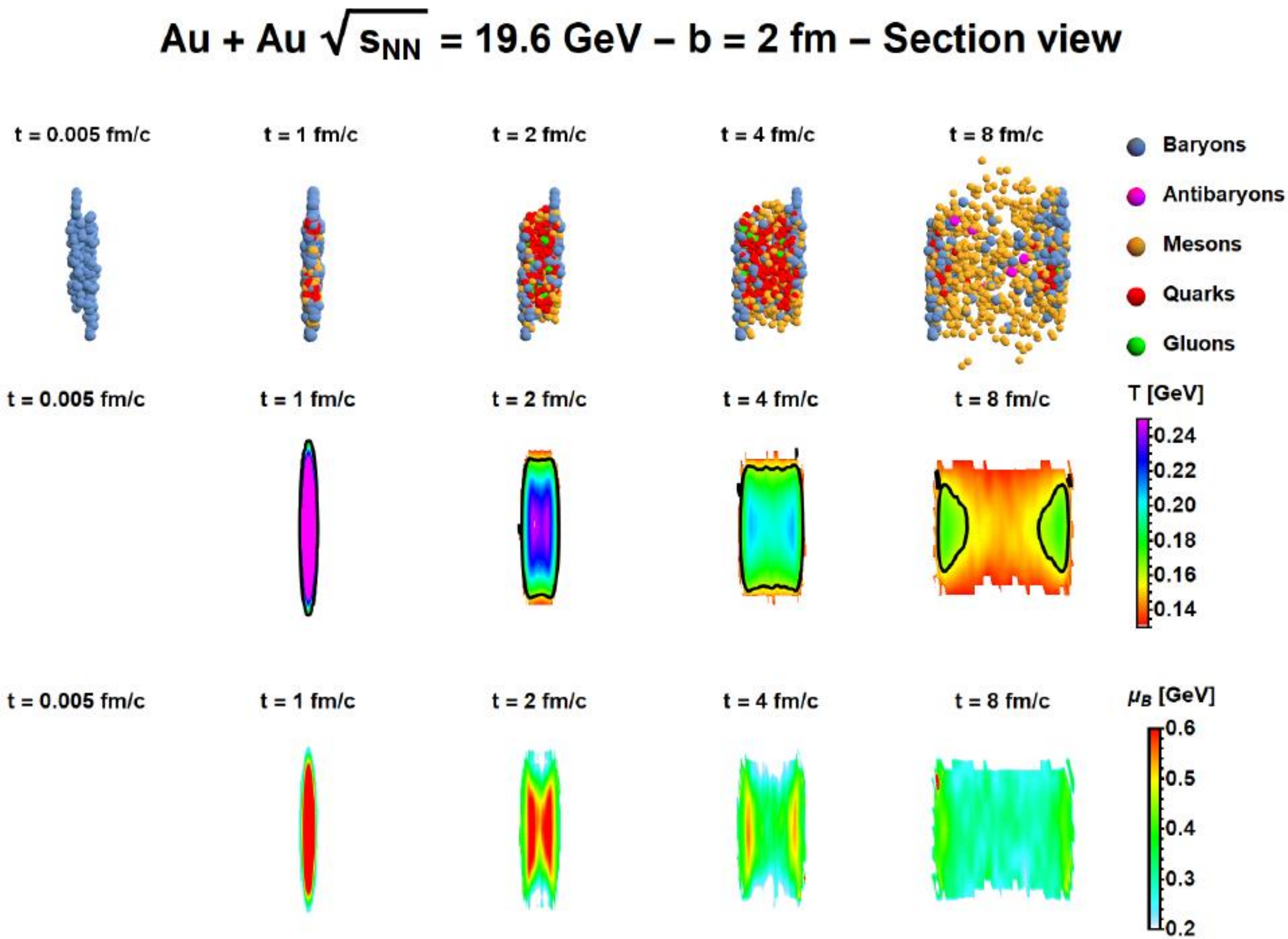

Illustration for a HIC ($\sqrt{s_{NN}} = 17$ GeV)

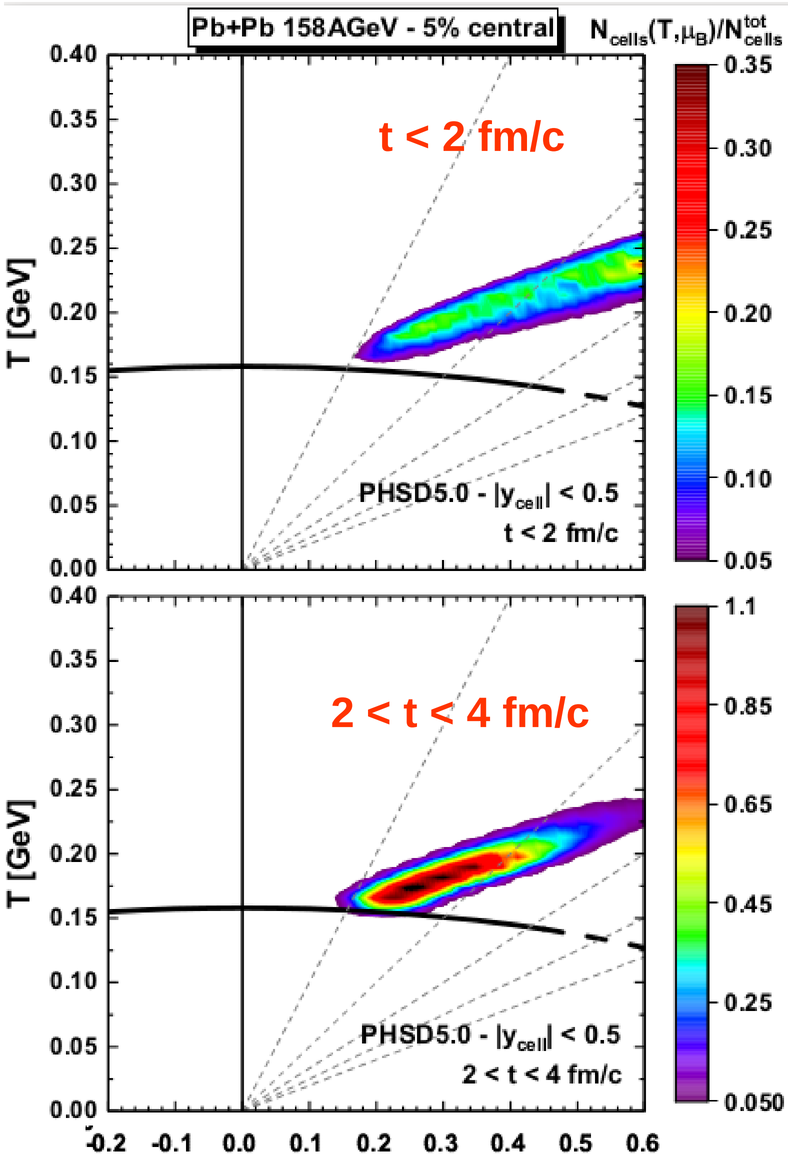

Distribution of cells ($|y_{cell}|$<0.5) with T>T_C

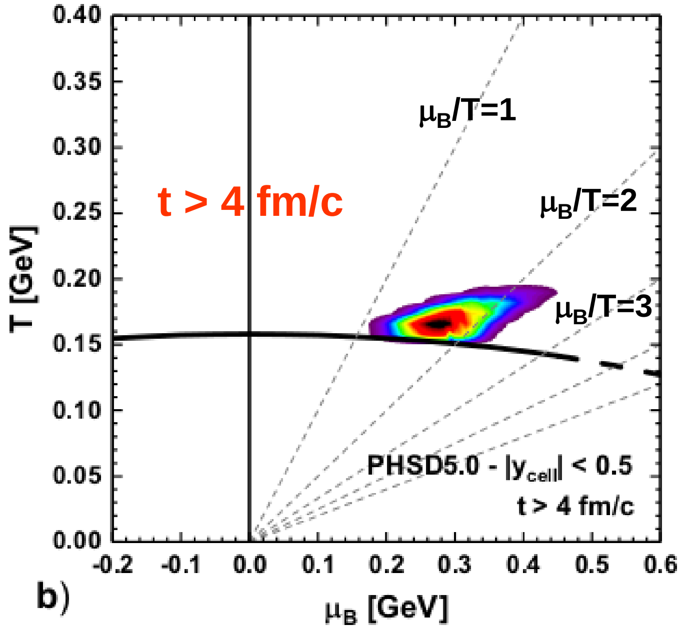

P. Moreau et al., PRC100 (2019) 014911

Results for HICs from PHSD 4.0 and 5.0

- **Comparison between three different results:**

1) **PHSD 4.0 : only $\sigma(T)$ and $\rho(T)$**

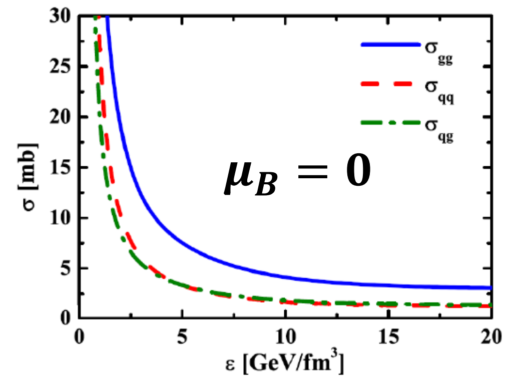

$\sigma(T)$ – parton interaction cross sections
$\rho(T)$ – spectral function of partons
➔ (masses and widths)

2) **PHSD 5.0 : with $\sigma\left(\sqrt{s}, m_1, m_2, T, \underline{\mu_B = 0}\right)$ and $\rho(T, \mu_B = 0)$**

In v.5.0: + angular dependence of diff. partonic cross sections

3) **PHSD 5.0 : with $\sigma\left(\sqrt{s}, m_1, m_2, T, \mu_B\right)$ and $\rho\ (T, \mu_B)$**

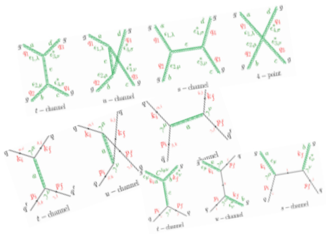

P. Moreau et al., PRC100 (2019) 014911

Results for HICs ($\sqrt{s_{NN}} = 200$ GeV)

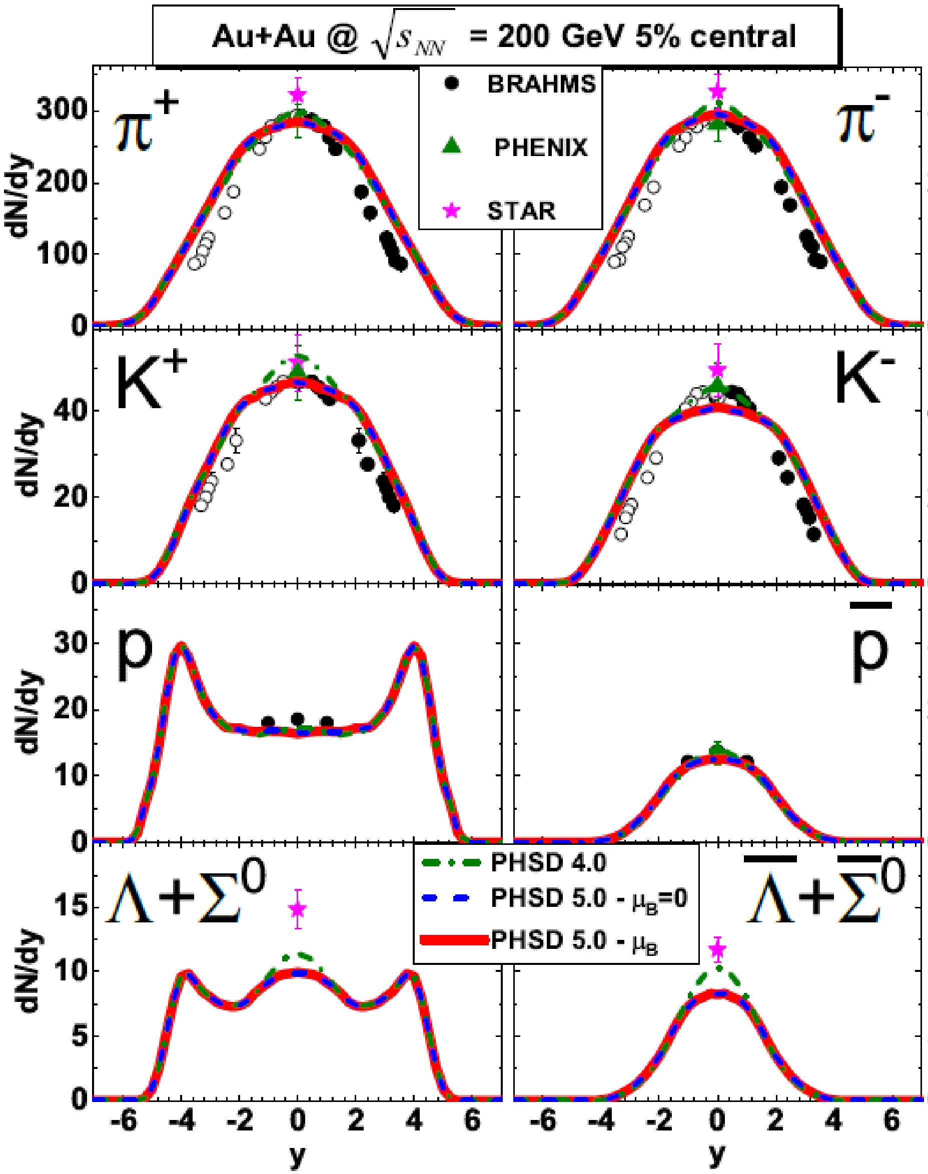

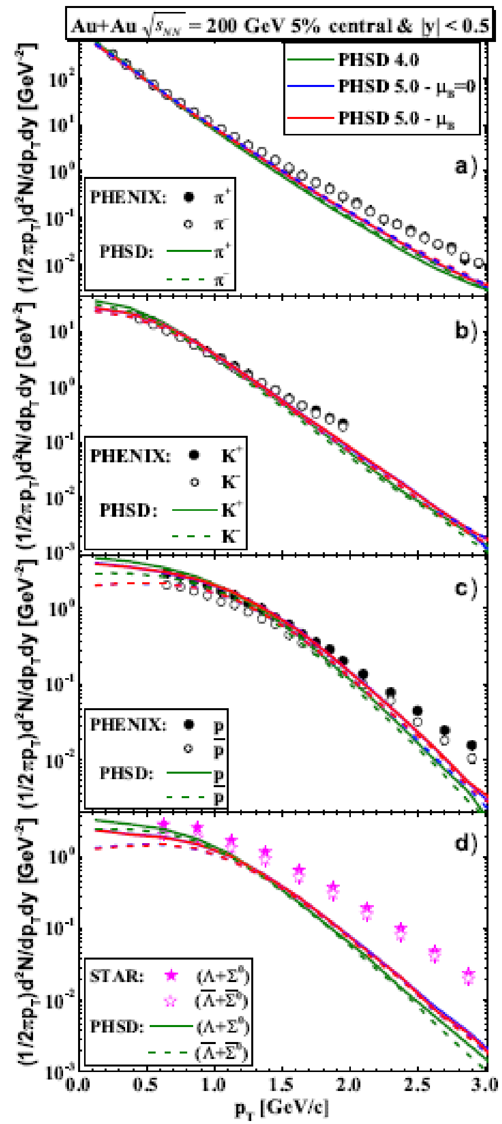

P. Moreau et al., PRC100 (2019) 014911

Results for HICs ($\sqrt{s_{NN}} = 17$ GeV)

High-μ_B regions are probed at low $\sqrt{s_{NN}}$ or high rapidity regions
But, QGP fraction is small at low $\sqrt{s_{NN}}$

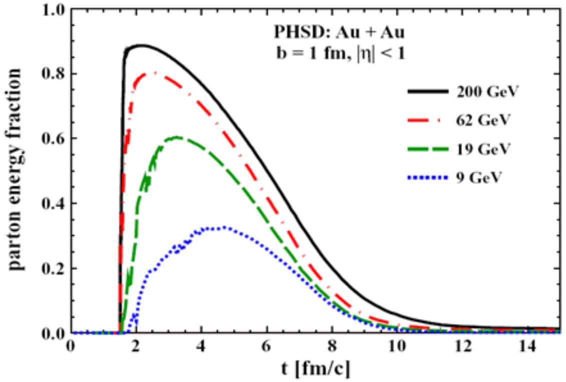

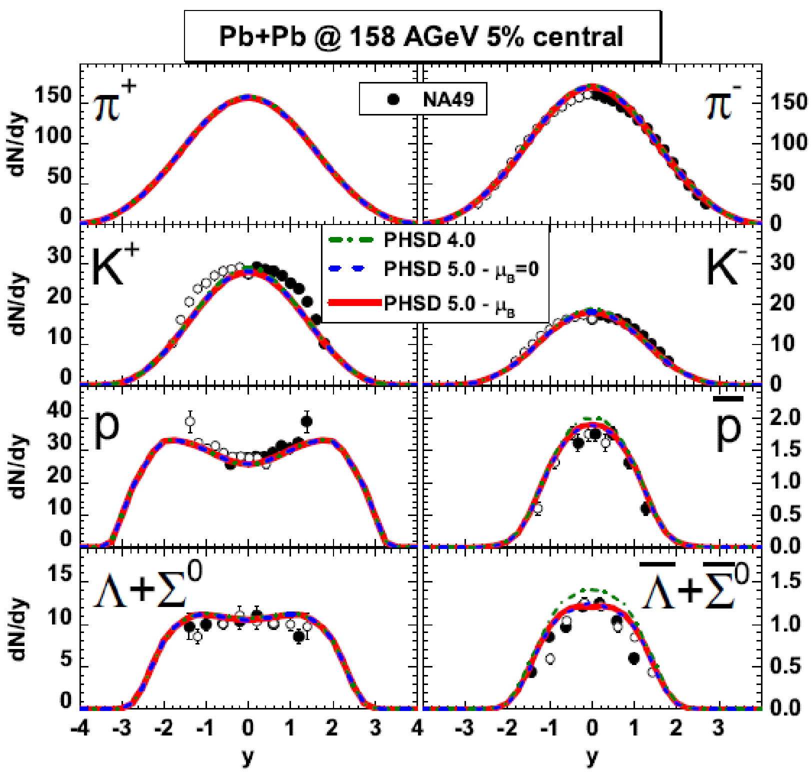

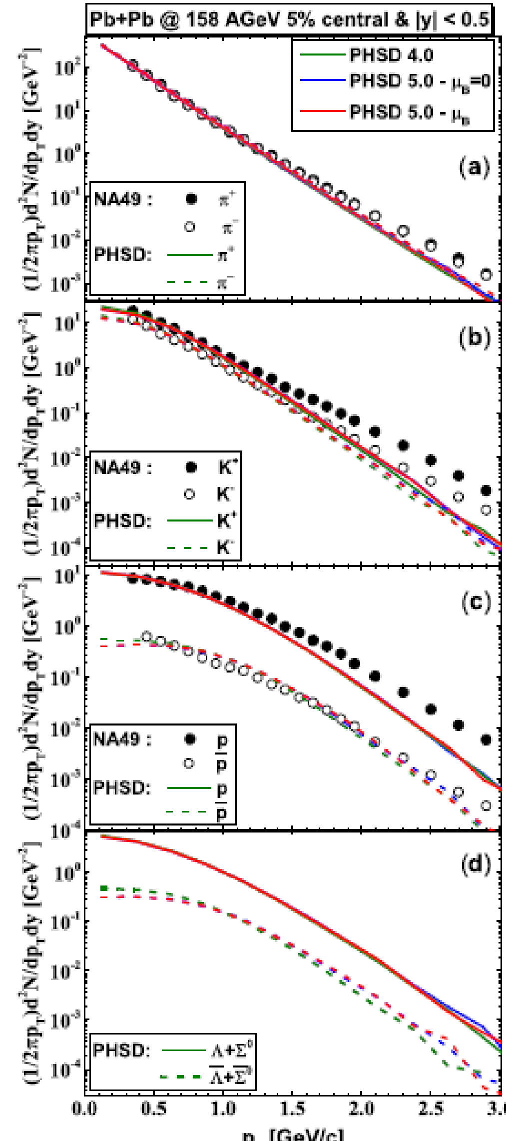

P. Moreau et al., PRC100 (2019) 014911

Results for HICs ($\sqrt{s_{NN}} = 7.6$ GeV)

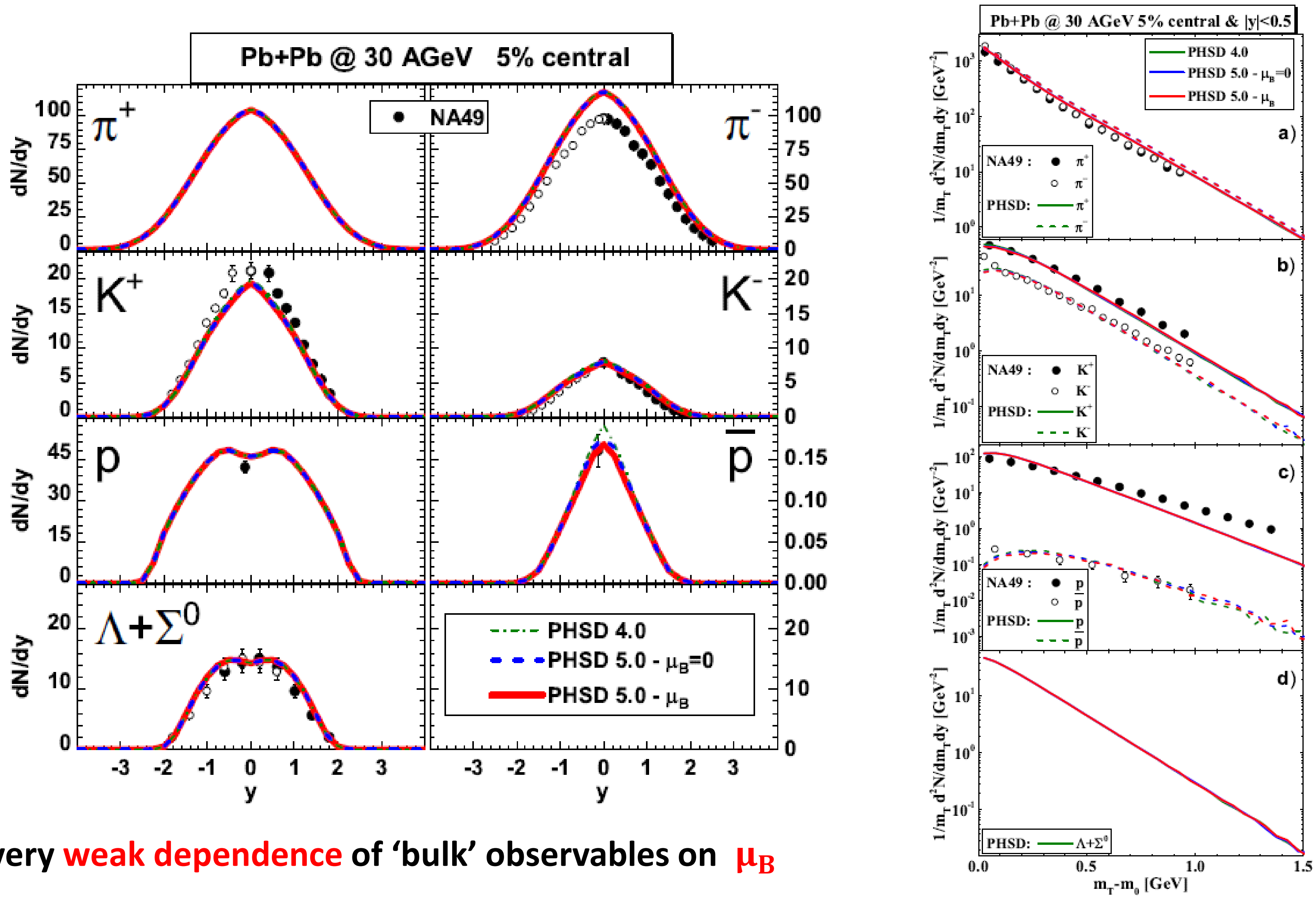

- very weak dependence of 'bulk' observables on μ_B

P. Moreau et al., PRC100 (2019) 014911

Results for HICs ($\sqrt{s_{NN}} = 4.86$ GeV)

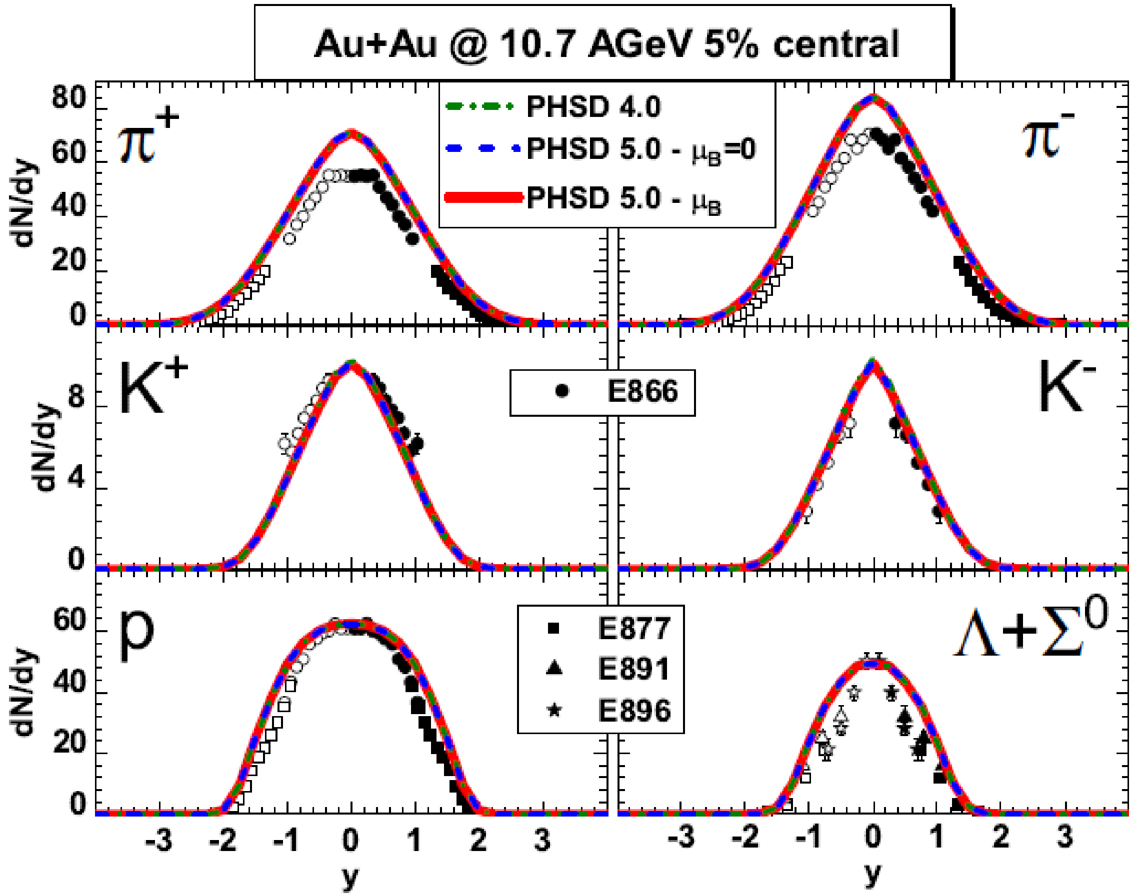

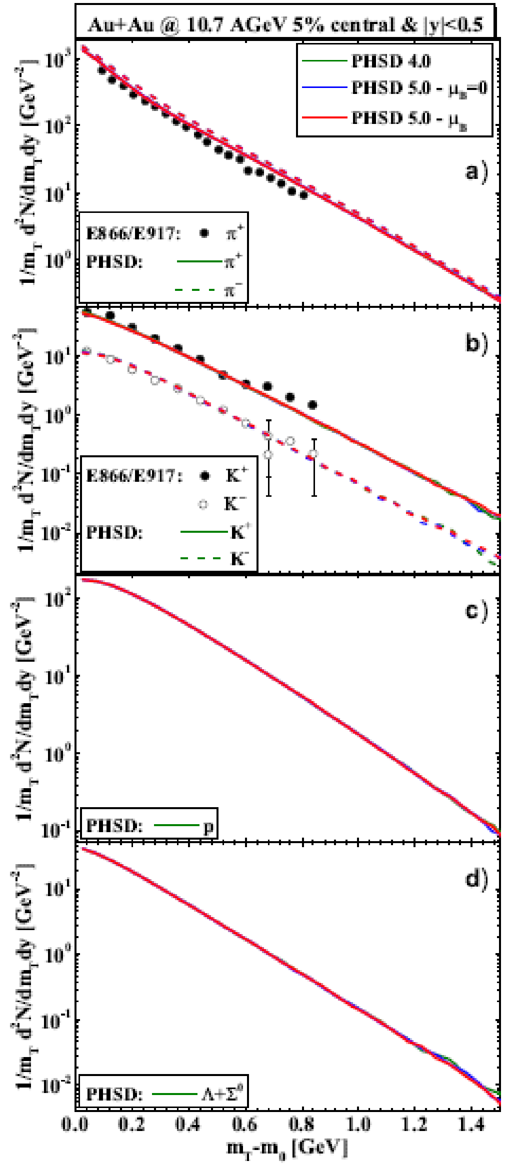

- very weak dependence of 'bulk' observables on μ_B

P. Moreau et al., PRC100 (2019) 014911

Elliptic flow v_2 ($\sqrt{s_{NN}} = 200\ GeV\ vs\ 27 GeV$)

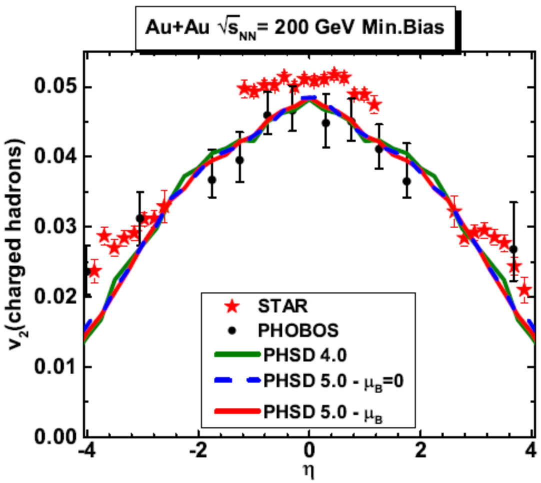

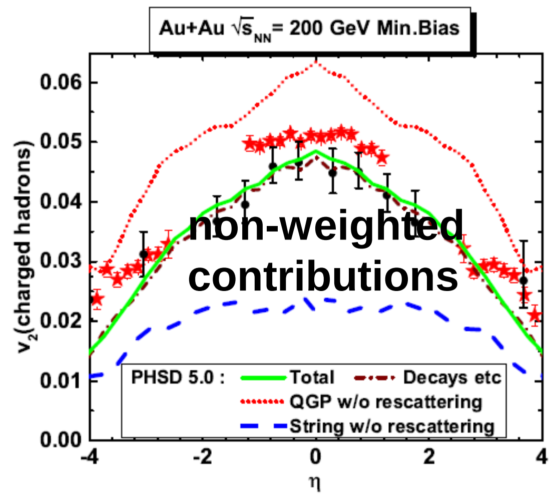

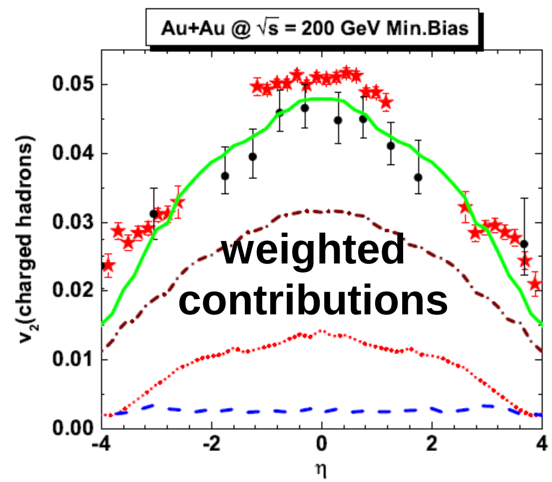

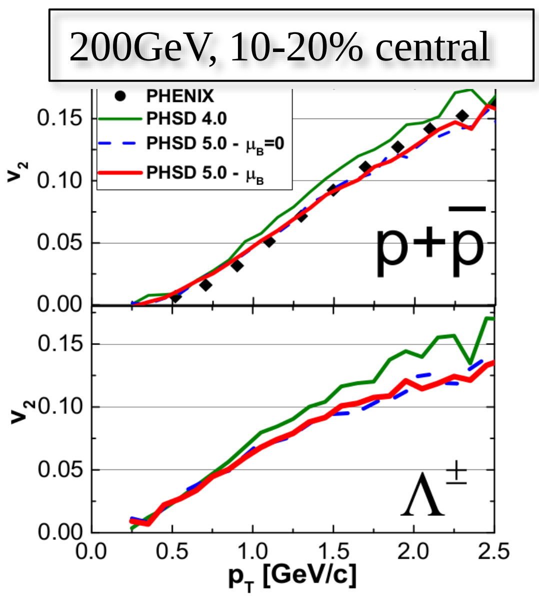

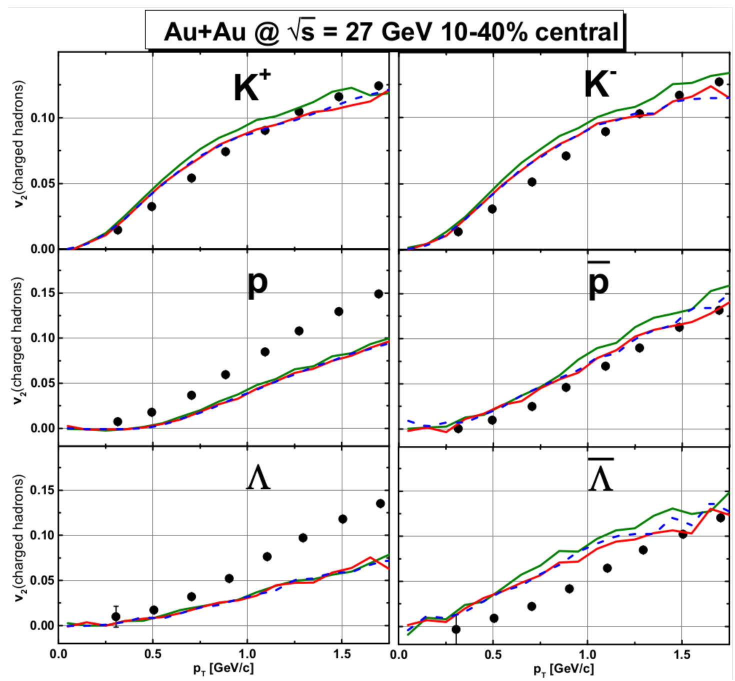

➔ **Small effect of μ_B dependence on v_2**

O. Soloveva et al., arXiv:2001.07951, MDPI Particles 2020, 3, 178

Results for v_1 for HICs ($\sqrt{s_{NN}} = 27$ GeV)

v_1

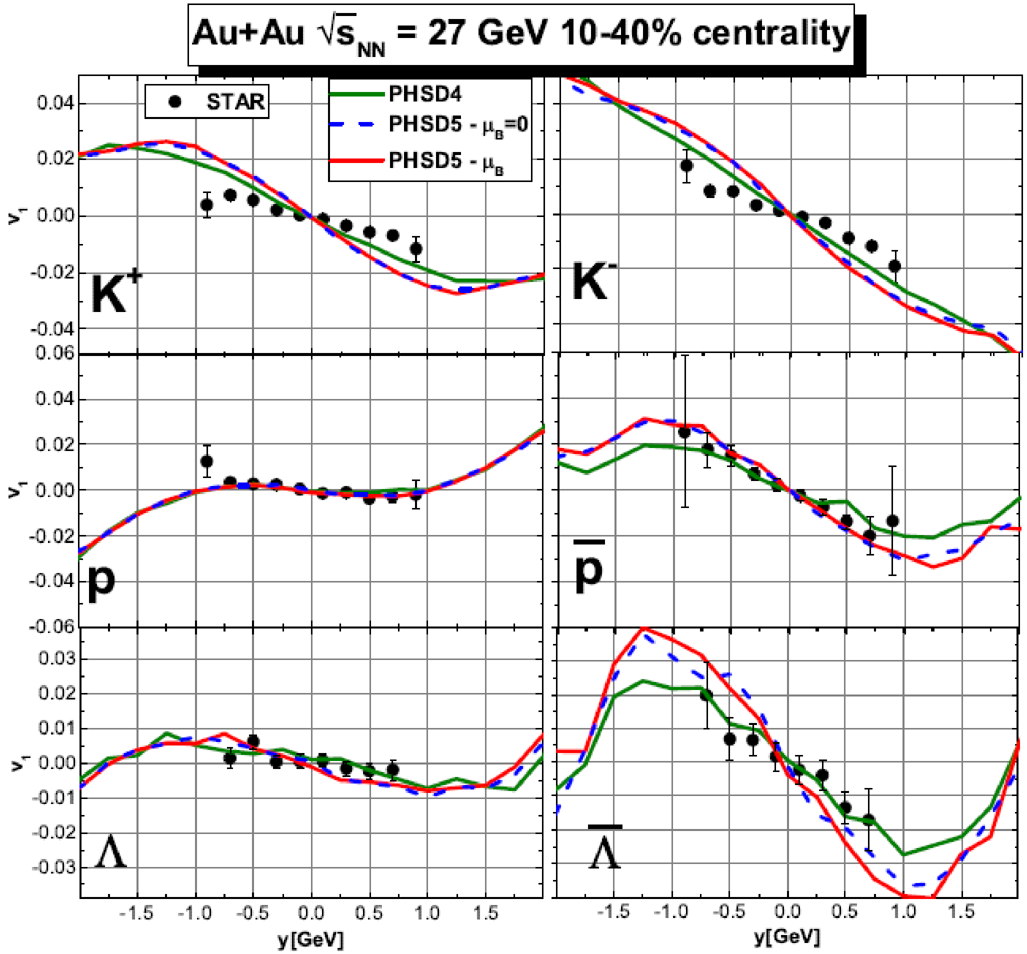

Messages from v_1, v_2 analysis:

- **weak dependence** of v_1, v_2 on μ_B
- **small influence** on v_1, v_2 of explicit $\sqrt{s}$ **-dependence** of total partonic cross sections σ + **angular dependence** of dσ/dcosθ due to the relatively **small QGP volume**
- strong **flavor dependence** of v_1, v_2

O. Soloveva et al., arXiv:2001.07951, MDPI Particles 2020, 3, 178

Messages from studies of QGP at T,μ_B

- (T,μ_B)-dependent partonic cross sections and masses/widths of quarks and gluons have been implemented in PHSD
- High-μ_B region is probed at low bombarding energies or high rapidity regions
- But, QGP fraction is small at low bombarding energies:
  ➔ no effects of (T,μ_B)-dependent partonic cross sections and masses/widths seen in 'bulk' observables – dN/dy, p_T-spectra
- Flow harmonics v_1, v_2 show :
  visible sensitivity to the explicit $\sqrt{s}$ -dependence of total partonic cross sections σ + angular dependence of dσ/dcosθ, however, weak dependence on μ_B

- **Outlook:**
  - More precise EoS at large μ_B
  - Possible 1st order phase transition at even larger μ_B?!

High-μ_B region of QCD phase diagram ➔ challenge for FAIR, NICA, BES RHIC

Thanks to: PHSD group - 2021

GSI & Frankfurt University
Olga Soloveva, Taesoo Song, Lucia Oliva,
Gabriele Coci, Ilia Grishmanovskii, Elena Bratkovskaya

Giessen University: Wolfgang Cassing

Former group members:
Olena Linnyk
Vitalii Ozvenchuk
Volodya Konchakovski
Hamza Berrehrah
Rudy Marty
Pierre Moreau
Thorsten Steinert
Alessia Palmese
Eduard Seifert
Andrej Ilner
Daniel Cabrera

Collaborations:

Frankfurt University:
Carsten Greiner, Juan Torres-Rincon

SUBATECH, Nantes University:
Jörg Aichelin, Pol-Bernard Gossiaux,
Marlene Nahrgang, Klaus Werner

JINR, Dubna:
Vadim Voronyuk, Viktor Kireev

Barcelona University:
Laura Tolos

Duke University:
Steffen Bass, Pierre Moreau

Catania University:
Vincenzo Greco

PHSD home page:
http://theory.gsi.de/~ebratkov/phsd-project/PHSD/index1.html